Flavour Changing Charged Current Within and Beyond the Standard Model

Rahat Ashraf
Regn.# 203160

A thesis submitted in partial fulfillment of the requirements
for the degree of **Master of Science**
in
Physics

Supervised by: Dr. Muhammad Ali Paracha
Co-Supervised by: Dr. Ishtiaq Ahmed

School of Natural Sciences
National University of Sciences and Technology
H-12, Islamabad, Pakistan

Year 2021

FORM TH-4

National University of Sciences & Technology

MS THESIS WORK

We hereby recommend that the dissertation prepared under our supervision by: Rahat Ashraf, Regn No. 00000203160 Titled: **Flavour Changing Chargded Current Within and Beyond the Standard Model** accepted in partial fulfillment of the requirements for the award of **MS** degree.

Examination Committee Members

1. Name: Dr. Rizwan Khalid Signature:

2. Name: Dr. Muddasir Ali Shah Signature:

External Examiner: Dr. Muhammad Jamil Aslam Signature:

Supervisor's Name Dr. Muhammad Ali Paracha Signature:

Co-Supervisor's Name Dr. Ishtiaq Ahmed Signature:

Head of Department

31/5/2021
Date

COUNTERSINGED

Date: 01/06/2021

Dean/Principal

Dedication

To my parents

They have always been a source of hope, motivation and endurance to pursue higher education,

and to meet the conditions of life with passion and excitement.

Acknowledgements

In the name of Allah Almighty, the Most Benevolent,Gracious and the Most Merciful. All favour be to Allah Almighty, the Lord of both world, whose bounties are unbounded, whose benevolence is overlasting enabled me to perceive and pursue ideas, and may prayers and peace be upon our Prophet Muhammad (P.B.U.H).

First, I would like to share my sincere appreciation and strong sense of honor to my *supervisor*, *Dr. Muhammad Ali Paracha*, is a enterprising, ethical and competent instructor, who always inspire and support me with his expertise. His timely suggestion, with kindness, ambition and solidity, made it possible for me to frame this dissertation into its final form.

My special admiration, warmth, and recognition to my *Co-Supervisor*, *Dr. Ishtiaq Ahmed*, and *Dr. Abdur Rehman*, who made my research victorious and assisted me at every point to meet my goal. The advice and encouragement earned from him is crucial to the progress of this dissertation.

My heartfelt thanks to the leaders of my Advisory Committee, *Dr. Rizwan Khalid*, *Dr. Muddasir Ali Shah* and *Dr. Saadi* for their encouragement and help for enhancing my research work.

I would like to take this pledge and say thank you so much to all my mates, Saba Asghar, Saira Parveen, Mahnoor Mirza, Ruttab Nadeem, Sundas gul, Jameela Fathima, Fatima shahid, Ayesha Zaheer, Zeeshan Rasheed, M Usman, Danish Ali Hamza, Zaheer Ud Din Babar and Ahzaz Jadoon for their support and encouragement.

The righteous credit ends up going to my family. For their indefinite love and endless dua I am always owed to my parents. I warmly appreciate their encouragement and firm support for me.

Rahat Ashraf

Abstract

We study $B \to D\tau\bar{\nu}_\tau$ and $B \to D^*\tau\bar{\nu}_\tau$ flavour changing charged current decay processes. These processes are interesting due to having persistent anomalies, R_D and R_{D^*}, first reported by Belle in 2007 and later by the different experiment like LHCb, Belle and BABAR. These anomalies hint physics beyond-the-Standard Model that is commonly named as new physics. For theoretical framework to study these transitions, for all possible dimension-six operators including new physics in model independent way, we write a low-energy effective Hamiltonian. We used the Wilson coefficients that are obtained from a numerical fit to all existing data to predict our observables. For numerical predictions we used HQET form factors for both transitions. We focus on $B \to D^*\tau\bar{\nu}$ decay that provides interesting angular observables due to cascade decay of $D^* \to D\pi$. Within and beyond the standard model our findings match with the known results in model independent way for angular observables.

Contents

List of Figures

Chapter 1

Introduction

This thesis is based on the Standard Model (SM) [1–16] and beyond. The SM outline our present knowledge of the three fundamental non-gravitational forces: strong, electromagnetic and weak. It is incredible that all these three forces are based on a common principle of gauge invariance. The main component of the SM is electroweak symmetry breaking (EWSB) mechanism occurring at the scale $v \sim 248$ GeV. The scale v corresponds to the vacuum-expectation-value (vev) of the Higgs doublet that provides masses to the weak bosons $W^{\pm}$ and Z^0, leaving the spinless boson H^0 (Higgs) as the physical degree of freedom. The SM emerged as a complete theory in 2012 in the sense that its last missing Higgs particle H^0 was experimentally found with mass around 126 GeV [17, 18]. In the next chapter 2, we will present the details on the SM.

The B meson has developed a framework for studying the SM and for exploring the New Physics (NP) effects at low-energy scales both at theoretical and experimental levels.

In the present work, we focus on the quark flavour sector in the context of a subclass of B-meson flavour-changing-charged-current (FCCC) [see Sec. 2.2] semileptonic decays specifically,

$$B^+(\bar{b}u) \to \bar{D}^0(\bar{c}u)l^+\nu_l, \qquad B^+(\bar{b}u) \to \bar{D}^{*0}(\bar{c}u)l^+\nu_l \tag{1.1}$$

and

$$B^0(\bar{b}d) \to D^-(\bar{c}d)l^+\nu_l, \qquad B^0(\bar{b}d) \to D^{*-}(\bar{c}d)l^+\nu_l, \tag{1.2}$$

here l stands for (e), (μ) and (τ) leptons. At quark level they are represented as $\bar{b} \to \bar{c}l^+\nu_l$, see Fig. 1.1. However, for brevity through out this thesis we will use $B \to D\tau\bar{\nu}$ and $B \to D^*\tau\bar{\nu}$ and $b \to cl\overline{\nu}_l$. In these exclusive decay processes both the flavour and charge will be changed as the b quark is converted to a c quark by the weak current that causes a factor of CKM matrix element $\vee_{cb}$ (see Sec. 2.3) in the amplitude. The SM parameter $|\vee_{cb}|$ can be extracted precisely using these decays. There are two directions are for the determination of CKM matrix component, namely inclusive and exclusive final states. It is shown in Fig. 1.1 that in this process $b \to c$

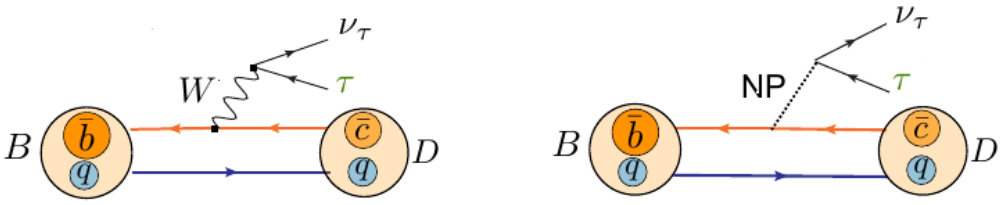

Figure 1.1: $\bar{b} \to \bar{c}\tau^+\nu$ processes in the SM (left) and possible beyond the SM (right). And, q in graphs represents u, and d quarks see, Eqs. 1.1 and 1.2. [19]

the new physics NP effect potentially comparable with the tree-level contribution of the SM. These processes are appealing and compelling due to the reason that they have anomalies since 2007 in the following R_D and R_{D^*} observables that are defined as,

$$R_D \equiv \frac{\mathcal{B}(B \to D\tau\overline{\nu}_\tau)}{\mathcal{B}(B \to Dl\overline{\nu}_l)}, \qquad R_{D^*} \equiv \frac{\mathcal{B}(B \to D^*\tau\overline{\nu}_\tau)}{\mathcal{B}(B \to D^*l\overline{\nu}_l)}, \tag{1.3}$$

where l in Eqs. 1.3 stands for electron (e) and muon (μ). The $\mathcal{B}(B \to D\tau\overline{\nu}_\tau)$ encodes the branching ratio for $B \to D\tau\overline{\nu}_\tau$ decay. The CKM matrix element $|\vee_{cb}|$ cancell in these ratios so they are independent of $|\vee_{cb}|$, but these ratios depend on the non-perturbative form factors over the entire kinematic range, $(m_l)^2 < q^2 < (M_B - m_{D^{(*)}})^2$, with the massless neutrinos. As mentioned above, in these anomalies physicist look for physics BSM. We consider NP in a model independent way present our work, see

Eq. 4.1 of chapter 4. The SM predictions, performed by several groups [20–23], are averaged by Heavy Flavour Averaging Group (HFLAV) [24] for these ratios are given as,

$$R_D^{\rm SM} = 0.299 \pm 0.003, \qquad R_{D^*}^{\rm SM} = 0.258 \pm 0.005. \tag{1.4}$$

The first measurment of semitauonic B decays was by Belle [25] in 2007, with succeeding measurments by Belle [26–29], BaBar [30], and LHCb [31,32]. The average values by HFLAV [24] of the experimental results read as,

$$R_D^{\rm exp} = 0.407 \pm 0.039 \pm 0.024, \qquad R_{D^*}^{\rm exp} = 0.306 \pm 0.013 \pm 0.007, \tag{1.5}$$

Here the first is statistical and second is systematical uncertainty. However, the latest Belle measurement brings down to the world average discrepancy from 3.8σ (HLFAV 2018) to 3.1σ (HFLAV 2019) that is shown in Fig. 1.2.

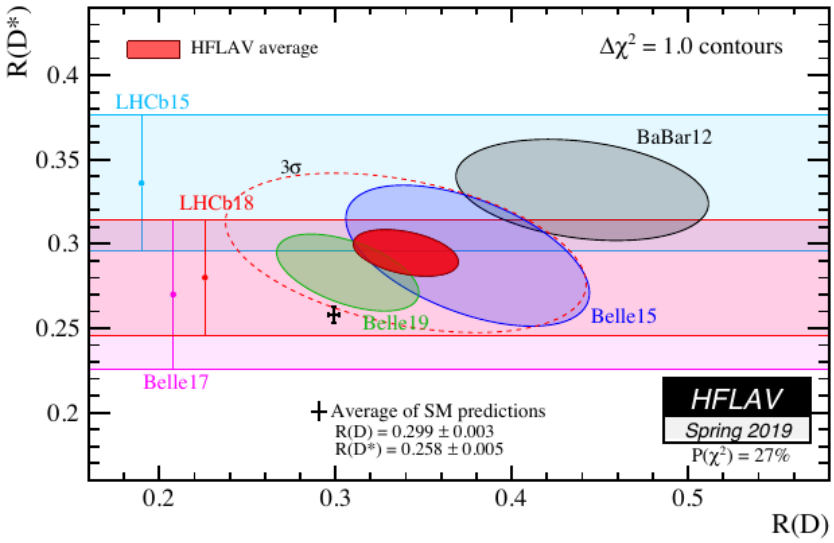

Figure 1.2: Current status of R_D and R_{D^*}. Latest Belle measurement brings down to the world average discrepancy from 3.8σ (HFLAV 2018) to 3.1σ [19].

For theoretical framework to study these transitions, we use an effective field theory approach discussed at length in chapter 3. Including new physics, we write down a low-energy effective Hamiltonian. In chapter 4, we start with this Hamiltonian and

subsequently, we write down the differential decay distribution for decay processes under consideration of this thesis. We use the heavy quark effective theory (HQET) parametrization for the $B \to D$ and $B \to D^*$ transition form factors. Moreover, to predict our observables we use the Wilson coefficients appear in the effective Hamiltonian that are obtained from a numerical fit to all existing data.

The thesis consists of four chapters that are organized as follows. In Chapter 2 we have reviewed the SM of particle physics in detail. Chapter 3 is devoted to a comprehensive analysis of the theoretical framework for B-decays. In Chapter 4, the $b \to c\tau\overline{\nu}_\tau$ process and its phenomenology are discussed. At the end, we conclude in Chapter 5.

Chapter 2

The Standard Model of elementary particle physics

The SM is an impressive theoretical achievement Despite its success, one should keep in mind that the SM is likely only an effective theory that describes Nature at low energies, at or below the EWSB scale ($v \sim 248$ GeV). At higher energies, BSM degrees of freedom may become dynamical. Their possible existence could help us in better understanding the EWSB mechanism, neutrino masses and mixings, A search for BSM theories is actively being carried out in two complementary ways, namely via direct production searches (high energy frontier) and via indirect searches (high intensity frontier). Both approaches require sincere theoretical predictions with quantifiable error estimates. In both of them, an important issue is to keep quantum effects under control, particularly the QCD ones. The main purpose of the Large Hadron Collider (LHC) are the direct searches at the TeV scale and beyond. At the same time, low energy measurements are becoming progressively accurate, increasing their potential of indirect searches. This requires higher precision on the theoretical side. In many cases, higher-order perturbative quantum corrections need to be calculated. It is particularly relevant for processes where virtual exotic particles might contribute to loop amplitudes.

The gauge theory of the SM is based on $SU(3)_C \times SU(2)_L \times U(1)_Y$ gauge group and

its contents are given in Tab. 4.1. We will used $SU(3)_C \times SU(2)_L \times U(1)_Y$ unanimously as $SU(3) \times SU(2) \times U(1)$ in this thesis. In electroweak theory, a chiral particle (fermion) can be defined with two elements as left and right components as,

$$\varphi = \varphi_L + \varphi_R. \tag{2.1}$$

Component of φ can be find by the operation of projection operator,

$$\varphi_L = P_L \varphi, \qquad \varphi_R = P_R \varphi, \qquad P_{L,R} = \frac{1}{2}(1 \pm \gamma_5). \tag{2.2}$$

Within the SM, for the vacuum expectation value of Higgs doublet H, the $SU(2) \otimes U(1)$ symmetry is spontaneously broken.

$$SU(3)_C \otimes SU(2)_L \otimes U(1)_Y \xrightarrow{SSB} SU(3)_C \otimes U(1)_{QED} \tag{2.3}$$

where SSB stands for Spontaneous symmetry breaking. This spontaneous break of $SU(2) \otimes U(1)$ gives mass to the gauge bosons $W^{\pm}$ and Z^0. The generators of the the electroweak gauge group are related to electric charge Q by Gell-Mann-Nishijima formula and Q remain conserved,

$$Q = I_3 + Y. \tag{2.4}$$

The flavour structure of the SM is dictated by the Higgs-quark-antiquark Yukawa interactions which generate the quark masses. The Yukawa coupling matrices contain a sizeable number of independent parameters. The CKM matrix describes the quark mass eigenstate mixing under weak interactions. See Sec. 2.3 for details on CKM matrix. We review in detail the SM ingredients mentioned above in what follows to this chapter.

Table 2.1: Matter fields in the standard model

Field	$SU(3)_C$	$SU(2)_L$	$U(1)$
$Q_L^i = \begin{pmatrix} u_L^i \\ d_L^i \end{pmatrix}$	3	2	1/6
u_R^i	3	1	2/3
d_R^i	3	1	-1/3
$L_L^i = \begin{pmatrix} \nu_L^i \\ e_L^i \end{pmatrix}$	1	2	-1/2
e_R^i	1	1	-1
$H = \begin{pmatrix} H^+ \\ H^0 \end{pmatrix}$	1	2	1/2

[1]The i index label the families of leptons and quarks. [**?**]

2.1 Standard Model Lagrangian

The SM lagrangian reads as,

$$\mathcal{L}_{SM} = \mathcal{L}_{Yukawa} + \mathcal{L}_{Higgs} + \mathcal{L}_{kin}, \tag{2.5}$$

where $\mathcal{L}_{kin}$, $\mathcal{L}_{Higgs}$ and $\mathcal{L}_{Yukawa}$ are given in equations 2.12, 2.13 and 2.24, respectively. To slightly talk about gauge invariance, let us take free Dirac Langrangian that is defined as,

$$\mathcal{L} = \overline{\varphi}(i\gamma^\mu \partial_\mu - m)\varphi. \tag{2.6}$$

This Langrangian is invariant in the global gauge transformation,

$$\varphi(x) \to e^{i\alpha}\varphi(x); \quad \overline{\varphi}(x) \to e^{-i\alpha}\overline{\varphi}(x), \tag{2.7}$$

where phase $i\alpha$ is independent of space time position x. Local gauge invariance refers to invariance with $i\alpha(x)$ phases that are dependent at every spacetime level,

$$\varphi(x) \to \varphi'(x) = \exp^{i\alpha(x)}\varphi(x), \ \overline{\varphi}(x) \to \overline{\varphi'}(x) = e^{-i\alpha(x)}\overline{\varphi}(x). \tag{2.8}$$

Above Langrangian does not hold local gauge invariance. Therefore, a certain gauge field corresponding to each symmetrical group will be added for gauge invariance. Here a Covariant derivative D_μ will be used for symmetry requirement. So $\partial_\mu \rightarrow D_\mu$ and it is definable as,

$$D_\mu = \partial_\mu - ieqA_\mu, \tag{2.9}$$

here e is the coupling constant, q is the fermions charge and A_μ is the fermionic field, that is transformed as,

$$A_\mu \rightarrow A_{\mu'} = A_\mu - \frac{1}{e}\partial_\mu \alpha(x). \tag{2.10}$$

Yang-Mills extended the idea of local gauge invariance from $U(1)$ to $SU(2)$ symmetric transformation with two Dirac particles lying in $SU(2)$ doublet. In this case, covariant derivative is defined as

$$D_\mu \varphi = (\partial_\mu - ig_s G^a_\mu t^a - igW^i_\mu \tau^i - ig' B_\mu Y)\varphi, \tag{2.11}$$

where the second term $g_s G^a_\mu t^a$ indicate the strong interaction with strong coupling g_s, gluonic field $G^a_\mu$and $SU(3)$ generator t^a. The generator $t^a = 0$ for color singlet and $t^a = \frac{\lambda^a}{2}$ for color triplet, λ^a is Gell-Mann matrices. The third term $gW^i_\mu \tau$ covers the weak coupling (g), 3 gauge bosons W^i_μ and τ^i is the generator of $SU(2)$, for $SU(2)$ doublet $\tau^i = \frac{\sigma^i}{2}$, where σ^i is the Pauli Matrices and for $SU(2)$ singlet $\tau^i = 0$. In the fourth term Y represents the hypercharge, B^μ is the electromagnetic field and g' is the electromagnetic coupling.

The kinetic component of the SM Langrangian ($\mathcal{L}_{kin}$) introduced in Eq. 2.5 can be define as,

$$\mathcal{L}_{kin} = \overline{\varphi}_L (i\partial_\mu + \frac{1}{2} g_s G^a_\mu \lambda^a + \frac{1}{2} gW^i_\mu \sigma^i + \frac{1}{6} g' B_\mu)\varphi_L \tag{2.12}$$

The Higgs part of the SM lagrangian introduced in Eq. 2.5 reads,

$$\mathcal{L}_{higgs} = (D_\mu H)^\dagger (D^\mu H) - V(H), \tag{2.13}$$

where D is the covarient derivative introduce to produce gauge invariance under $SU(2)_L \times U(1)_Y$,

$$D_\mu = \partial_\mu - igW_\mu^i \tau^i - ig' B_\mu Y, \tag{2.14}$$

and $SU(2)$ doublet of the real scalar field H is,

$$H = \begin{pmatrix} H^+ \\ H^0 \end{pmatrix}, \tag{2.15}$$

and the Higgs potential $V(H)$ reads,

$$V(H) = -\mu^2 H^\dagger H + \lambda (H^\dagger H)^2 \tag{2.16}$$

In the Higgs potential, λ and μ are two couplings. At $\lambda > 0$, the grounded state is defined with two possibilities:

1. For $\mu^2 < 0$ the Higgs potential has minimum value at $H = 0$. It define mass of massive particle is associated with μ and the parabolic form of Higgs potential curve is obtained as in the fig. 2.1(right).

2. For $\mu^2 > 0$, the Higgs potential has non-zero minimum value through Higgs mechanism H acquires a vev, and we can use $SU(2)$ symmetry to rotate this expectation value into the standard form one 2.18. The shape obtained is a 'Mexican hat' curve for the potential as depicted in fig. 2.1(left). The minimum value of the potential is at,

$$H H^\dagger = \frac{\mu^2}{2\lambda} = \frac{\upsilon^2}{2}, \tag{2.17}$$

with absolute value of the ground state is,

$$\langle H \rangle = \begin{pmatrix} 0 \\ \upsilon/\sqrt{2} \end{pmatrix}, \text{with } \upsilon \text{ a real and positive number, } \upsilon = \sqrt{\frac{\mu^2}{\lambda}}. \tag{2.18}$$

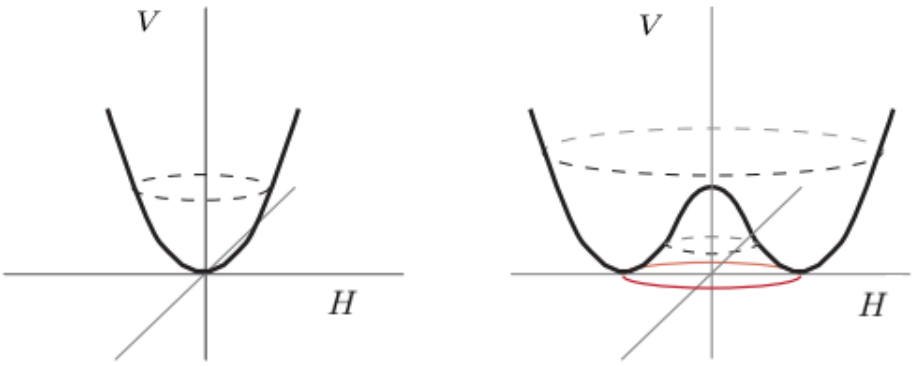

Figure 2.1: The potential corresponding with two different values of μ^2 [33]

At this vev symmetry breaks spontaneously, $SU(2)_L \otimes SU(1)_Y \xrightarrow{SSB} U(1)_{EM}$. According to the 'Goldston Theorem' three massless gauge bosons will become massive during the symmetry breaking in the Higgs field The scalar field in terms of unitary gauge are written as,

$$\begin{aligned}(D^\mu H)^\dagger (D_\mu H) &= \left| \begin{pmatrix} \partial_\mu - \frac{i}{2} g \sigma^i W_\mu^i - \frac{i}{2} g' Y B_\mu \end{pmatrix} \begin{pmatrix} 0 \\ \frac{\nu}{\sqrt{2}} \end{pmatrix} \right|^2 \\ &= \frac{\nu^2}{8} \left| \begin{pmatrix} \frac{g}{2} W_\mu^i \sigma^i + \frac{g'}{2} Y B_\mu \end{pmatrix} \begin{pmatrix} 0 \\ 1 \end{pmatrix} \right|^2 = \frac{\nu^2}{8} \left| \begin{pmatrix} g W_\mu^1 - i g W_\mu^2 \\ -g W_\mu^3 + g' B_\mu \end{pmatrix} \right|^2 .\end{aligned} \tag{2.19}$$

Gauge Field Masses: We can now evaluate the spontaneously generated mass terms for the $W^\pm$ and Z^0 by using Eq. 2.13,

$$\mathcal{L}_{gauge-boson-mass} = \frac{g^2 \nu}{8} (W_\mu^1 W_\mu^1 + W_\mu^2 W_\mu^2) + \frac{\nu^2}{8} (g W_\mu^3 - g' B_\mu), \tag{2.20}$$

where gauge bosons can be defined as,

$$W_\mu^\pm = \frac{W_\mu^1 \mp iW_\mu^2}{\sqrt{2}}, \qquad A_\mu = \frac{gW_\mu^3 + g'B_\mu}{\sqrt{g^2+g'^2}}, \qquad Z_\mu = \frac{gW_\mu^3 - g'B_\mu}{\sqrt{g^2+g'^2}}. \tag{2.21}$$

The masses of bosons are defined as,

$$M_W = \frac{g\nu}{2}, \qquad M_Z = \nu\frac{\sqrt{g^2+g'^2}}{2}, \qquad M_A = 0. \tag{2.22}$$

There are some important relations that we will use in this work that read as,

$$e = g\sin\theta_W = g'\cos\theta_W, \;\; g^2 = 4\sqrt{2}G_F m_W^2, \tag{2.23}$$

where G_F is Fermi constant used below Eq. 3.2 and θ_W is Weinberg angle or weak mixing angle. Its value is $\sin\theta_W^2 \sim 0.23$.

Fermion Masses: A fermionic mass term $\mathcal{L}_m = -m\overline{\varphi}\varphi = -m(\overline{\varphi}_L\varphi_R + \overline{\varphi}_R\varphi_L)$ is not allowed, because it causes an explicitly break of gauge symmetry. The fermion get masses from the interaction between Dirac field (φ) and scalar field (H) is known as Yukawa Coupling. So the Yukawa Langrangian is defined as,

$$\mathcal{L}_{Yukawa} = Y_{ij}\overline{\varphi}_L^i H\varphi_R^j + Y_{ij}^*\overline{\varphi}_R^j H^\dagger\varphi_L^i. \tag{2.24}$$

After EW symmetry breaking, masses of quarks and leptons are described by Langrangian in weak basis,

$$\mathcal{L}_{mass} = \overline{\varphi}_{iL}^{'u}M_{ij}^{'u}\varphi_{jR}^{'u} + \overline{\varphi}_{iL}^{'d}M_{ij}^{'d}\varphi_{jR}^{'d} + \overline{l}_{iL}^{'}M_{ij}^{'l}l_{jR}^{'} + h.c. \tag{2.25}$$

where mass matrices M_{ij} defined as

$$M_{ij}^{'u} \equiv \upsilon Y_{ij}^{'u} \quad M_{ij}^{'d} = \upsilon Y_{ij}^{'d} \quad M_{ij}^{'l} = \upsilon Y_{ij}^{'l}. \tag{2.26}$$

Generally, the Yukawa coupling and mass matrices are not diagonal. They can diagonalized by bi-unitary transformations as follows,

$$\begin{aligned} V_L^{u\dagger} M_{ij}^{\prime u} V_R^u &= diag(m_u, M_c, m_t) \equiv m_{ij}^u, \\ V_L^{d\dagger} M_{ij}^{\prime d} V_R^d &= diag(m_d, m_s, M_b) \equiv m_{ij}^d, \\ V_L^{l\dagger} M_{ij}^{\prime l} V_R^l &= diag(m_e, m_\mu, m_\tau) \equiv m_{ij}^l, \end{aligned} \tag{2.27}$$

where Vs are the unitary $(3 \otimes 3)$ matrix that are related to flavour (weak) and mass eigenstates as,

$$\varphi_L^u = V_L^u \varphi_L^{\prime u}, \quad \varphi_L^d = V_L^d \varphi_L^{\prime d}, \quad l_L = V_L^l \varphi_L^{\prime l}, \tag{2.28}$$

$$\varphi_R^u = V_R^u \varphi_R^{\prime u}, \quad \varphi_R^d = V_R^d \varphi_R^{\prime d}, \quad l_R = V_R^l \varphi_R^{\prime l}. \tag{2.29}$$

By using these transformations Langrangian becomes,

$$\mathcal{L}_{mass} = \overline{\varphi}_{iL}^u m_{ij}^u \varphi_{jR}^u + \overline{\varphi}_{iL}^d m_{ij}^d \varphi_{jR}^d + \bar{l}_{iL} m_{ij}^l l_{jR} + h.c., \tag{2.30}$$

and mass-term has been created. So the generalized form of the SM Langrangian in terms of Gauge bosons and field is,

$$\begin{aligned} \mathcal{L}_{\rm SM} &= \mathcal{L}_{kin} + \mathcal{L}_{Yukawa} + \mathcal{L}_{Higgs} \\ &= i\overline{\varphi}_L(\partial_\mu - \frac{i}{2} g_s \lambda^2 G_\mu^a - \frac{i}{2} g \sigma^i W_\mu^i - \frac{i}{6} g' B_\mu)\varphi_L \\ &+ Y_{ij} \overline{\varphi}_L^i H \varphi_R^j + (D_\mu H)^\dagger (D^\mu H) - V(H) + h.c. \, . \end{aligned} \tag{2.31}$$

In the context of physical fermions and bosons fields we will proceed the study of neutral and charged current.

2.2 Charged and Neutral Currents

Neutral Current: The interaction in which only flavour of the quark change but charge remain same are known as FCNC. See fig. 2.2 for FCNC vertices. An example of FCNC is $b \to sl^+l^-$. In the standard model FCNC is forbidden at tree level that is it only occurs at loop level in the SM. Flavour changing is due to different masses of quarks and when these quark move in the loop

Figure 2.2: Neutral current vertices describing the couplings of fermion pairs (quarks and leptons) to Z^0 boson.

Charged Current: The interaction in which both the flavour and charge will be

Figure 2.3: Charged current vertices describing the coupling of fermion pairs to vector boson $W^\pm$.

changed known as charged current. The Langrangian for the charged current reads,

$$\mathcal{L}_{CC} = -\frac{g}{\sqrt{2}}[W_\mu^+ \,\overline{\varphi}_{iL}^u \gamma^\mu (\vee_{\text{CKM}})_{ij} \varphi_{jL}^d + W_\mu^- \,\bar{l}_{iL} \gamma^\mu \nu_{li_L} + h.c.], \tag{2.32}$$

where $\vee_{\text{CKM}} = V_L^{u\dagger} V_L^d$ is the unitary matrix called CKM matrix. This is a 3×3 mixing

matrix element in the case of three quark generations,

$$\vee_{\rm CKM} = \begin{pmatrix} \vee_{ud} & \vee_{us} & \vee_{ub} \\ \vee_{cd} & \vee_{cs} & \vee_{cb} \\ \vee_{td} & \vee_{ts} & \vee_{tb} \end{pmatrix}. \tag{2.33}$$

For more details on CKM matric see Sec. 2.3. In the SM, weak charged currents interactions are occur at tree level that change the flavour. The FCCC process $b \to c\tau\overline{\nu}_\tau$ under our consideration belongs to this class. See fig. 2.3 for FCCC vertices.

2.3 CKM matrix and its parameterization

A central item in the Standard Model explaining flavour dynamics is the CKM matrix. [34, 35] The CKM matrix define mixing between three families of quarks in the SM such as,

$$\begin{pmatrix} d' \\ s' \\ b' \end{pmatrix} = \vee_{\rm CKM} \begin{pmatrix} d \\ s \\ b \end{pmatrix}, \tag{2.34}$$

where $\vee_{\rm CKM}$ is defined in Eq. 2.33. Here d', s', b' are the weak eigenstates and d, s, b are the mass (physical) eigenstates. The CKM matrix given in Eq. 2.33 has following parametrizations.

Standard parametrization: This parametrizes CKM matrix as,

$$\mathbf{V}_{\rm CKM} = \begin{pmatrix} c_{12}c_{13} & s_{12}c_{13} & s_{13}e^{-i\delta} \\ -s_{12}c_{23} - c_{12}s_{23}s_{13}e^{i\delta} & c_{12}s_{23} - s - 12s_{23}s_{13}e^{i\delta} & s_{23}c_{13} \\ s_{12}s_{23} - c_{12}c_{23}s_{13}e^{i\delta} & -c_{12}s_{23} - s_{12}c_{23}s_{13}e^{i\delta} & c_{23}c - 13 \end{pmatrix}, \tag{2.35}$$

where $c_{ij} = \cos\theta_{ij}$, $S_{ij} = \sin\theta_{ij}$. The above parametrization of V_{CKM} is defined by the product of three rotation matrix. Most experiments predicted that $\theta_{12} \gg \theta_{23} \gg \theta_{13}$ and $\delta \sim \mathcal{O}(1)$. Above parametrization depend on these three angles and one complex phase factor. Next we will discuss another parametrization that is called 'Wolfenstein Parametrization'.

Wolfenstein parametrization: This parametrization explains the off diagonal entities. In this parametrization, explicitly there are three real parameters (ζ, δ, A) and one imaginary parameter (η) in the $\vee_{\rm CKM}$ according to the Wolfenstein parametrization that is defined as,

$$\mathbf{V}_{\rm CKM} = \begin{pmatrix} 1 - \frac{\delta^2}{2} & \delta & A\delta^3(\zeta - i\eta) \\ -\delta & 1 - \frac{\delta^2}{2} & A\delta^2 \\ A\delta^3(1 - \zeta - i\eta) & -A\delta^2 & 1 \end{pmatrix} + \mathcal{O}(\delta^4). \tag{2.36}$$

This is widely useful approximation, mainly in B physics, This parametrization displays the unitarity condition of V_{CKM} as,

$$V^{\dagger}_{\rm CKM} \vee_{\rm CKM} = \mathbf{I} = \vee_{\rm CKM} V^{\dagger}_{\rm CKM}. \tag{2.37}$$

This implies that,

$$\Sigma_k V_{ik} V^*_{jk} = \delta_{ij} \qquad \text{and} \qquad \Sigma_k V_{kj} V^*_{ki} = \delta_{ij}. \tag{2.38}$$

By using above relation one finds,

$$\vee_{ud} V^*_{ub} + \vee_{cd} V^*_{cb} + \vee_{td} V^*_{tb} = 0 = \delta_{db}, \tag{2.39}$$

that depicts the unitary triangle shown in fig. 2.4. In this figure,

$$\alpha = arg\left(\frac{\vee_{cd}\vee^*_{cb}}{\vee_{td}\vee^*_{tb}}\right), \quad \beta = arg\left(\frac{\vee_{td}\vee^*_{tb}}{\vee_{ud}\vee^*_{ub}}\right), \quad \gamma = arg\left(\frac{\vee_{ud}\vee^*_{ub}}{\vee_{cd}\vee^*_{cb}}\right), \tag{2.40}$$

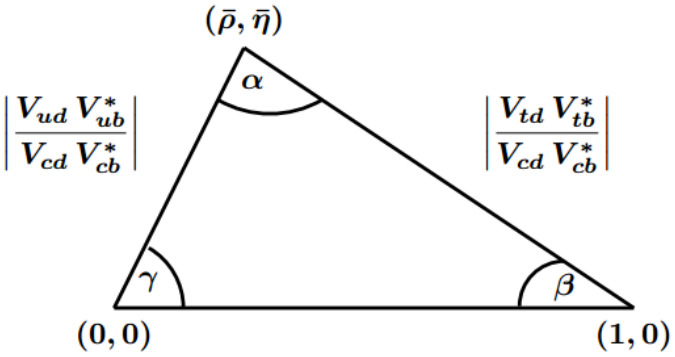

Figure 2.4: The CKM unitary triangle in $(\overline{\zeta}, \overline{\eta})$ plane. [34]

are the angles of this triangle. It is worth to mention that there is no analogue of the CKM matrix in the leptonic sector as one can see in Eq. 2.32.

Chapter 3

Theoretical Framework for B-decays

In the present chapter, Sec. 3.1 covers the basic and technical aspects of setting up a low energy effective theory that is valid below the electroweak scale. We focus on its elements that are relevant to B physics in and beyond the SM NP in model independent way.

3.1 An Introduction to Effective Field Theory

The weak radiative B meson decays are generated by loop diagrams involving the electro-weak-scale particles (notably the W boson and the top quark). In consequence, one encounters QCD corrections that are enhanced by powers of logarithms $\ln(m_W^2/m_b^2)$. In fact, the QCD perturbation series turns out to be a series in powers of $(\alpha_s(M_b))^n\ (\alpha_s(m_W)\ln(m_W^2/m_b^2))^m$, with $n, m = 0, 1, 2, \ldots$. Given the numerical values of $\alpha_s(M_b) \sim 0.22$ and $\alpha_s(m_W)\ln(m_W^2/m_b^2) \sim 0.7$, it makes sense to treat these quantities as formally independent, and resum the series in the latter one, still working order-by-order in $\alpha_s(M_b)$. It can most conveniently be achieved by Renormalization Group Equations (RGE) [36] for the Wilson coefficients work as a tool for the

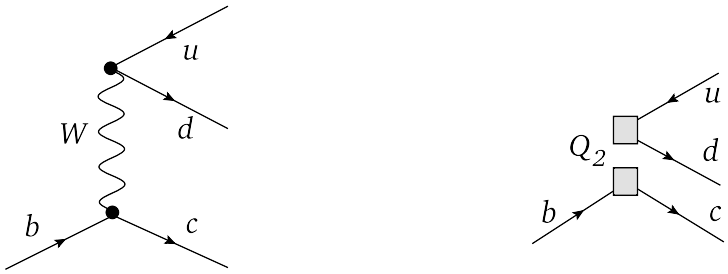

Figure 3.1: The LO $b \to cd\bar{u}$ process in the SM and in the low energy effective theory. Gray boxes show an insertion of one of the effective operators. [36]

large logarithm resummation.[1] In Sec. 3.1.1, the effective Lagrangian is constructed In perturbation theory, such a procedure can be thought about as an extension of the so-called decoupling theorem by Appelquist and Carazzone [37]. Once the effective Lagrangian is defined, we discuss the three necessary steps for evaluation of determining the matching and mixing in Sec. 3.1.2, and calculating the matrix elements in Sec.

3.1.1 The effective Lagrangian and operators basis

The core idea of OPE [38, 39] is a factorization of long- and short-distance physics. We shall begin with illustrating this idea using a simpler example. Let us consider a tree-level $b \to cd\bar{u}$ transition that is mediated by the W boson, as depicted in Fig. 3.1 (left). There are two reasons why we have chosen this very example for the sake of illustration. First, such a process is sensitive to QCD effects. Second, it involves quarks of four different flavours, so the number of relevant effective operators will be very limited. The amplitude corresponding to the LO Feynman diagram of this process in the SM reads (in the 't Hooft-Feynman gauge):

$$A = \left(\frac{-ig}{\sqrt{2}}\right)^2 \vee_{cb} V_{ud}^* \left(\bar{d}_L \gamma_\mu u_L\right) \frac{ig^{\mu\nu}}{m_W^2 - q^2} \left(\bar{c}_L \gamma_\nu b_L\right) \tag{3.1}$$

[1] Construction of effective theories and using the RGE is a general method for resummation of all sorts of large logarithms of scales that appear in physical amplitudes in Quantum Field Theory (QFT).

where $g = e/\sin\theta_W$ is weak coupling defined 2.23, and the maximum momentum transfer squared is $q^2_{max} = (M_b - M_c)^2$. Throughout the thesis, we treat the three lightest (u, d and s) quarks as massless. For brevity, we use identical notation for the quark fields and the corresponding Dirac spinors. Their left- and right- handed projections are denoted in the standard manner, i.e. $\varphi_{L,R} = P_{L,R}\,\varphi$, where $P_{L,R} = (1 \mp \gamma_5)/2$.

The W-boson mass $m_W \simeq 80$ GeV is over 16 times larger than $\sqrt{q^2} < M_b \sim 5\,\text{GeV}$, i.e. $q^2/m_W^2 < 0.004$. Thus, one can perform a Taylor expansion of the W-propagator into an infinite sum of local terms using $(1-x)^{-1} = \sum_{n=0}^{\infty} x^n$. Then the amplitude takes the form

$$A = -i\,2\sqrt{2}\,G_F\;\vee_{cb} V^*_{ud}\left(\bar{d}\,u\right)_{V-A}(\bar{c}\,b)_{V-A}\sum_{n=0}^{\infty}\frac{q^{2n}}{m_W^{2n}} \tag{3.2}$$

where $G_F = g_2^2/(4\sqrt{2}m_W^2)$ is the Fermi constant, and $(2\sqrt{2}G_F)^{-1/2} \simeq 174\,\text{GeV}$. The CKM matrix elements are denoted by V_{ij}, while $\left(\bar{d}\,u\right)_{V-A}$ stands for $\bar{d}_L\gamma_\mu u_L$ (and similarly for other flavours).

The r.h.s. of Eq. (3.2) can equivalently be obtained from the following LO effective weak interaction Lagrangian term:

$$\mathcal{L}_{\text{eff}} = -\frac{4G_F}{\sqrt{2}}\,\vee_{cb} V^*_{ud}\sum_{n=0}^{\infty}\frac{1}{m_W^{2n}}Q^{(n)}, \tag{3.3}$$

where the operators $Q^{(n)}$ are given (in position space) by

$$\left(\bar{d}\,u\right)_{V-A}\left[(-1)^n\Box^n\right](\bar{c}\,b)_{V-A} \tag{3.4}$$

with $\Box \equiv \partial^\alpha\partial_\alpha$ denoting the d'Alembertian. The dimensionality of the operators $Q^{(n)}$ in the units of mass is $6+2n$, i.e. $[Q^{(n)}] = 6+2n$. Due to the suppression of higher-n operators by inverse powers of m_W, the first term is a good approximation. In fact, higher-dimensional operators are practically always negligible from the phenomenolog-

ical standpoint in the SM analyses of FCNC processes.

From now on, we shall restrict to the dimension-six ($n = 0$) operators alone, assuming that it is sufficient for the required precision in our example. Taking into account possible generation of other operators at the dimension-six level, we write

$$\mathcal{L}_{\text{eff}} = \frac{4G_F}{\sqrt{2}} \vee_{cb} V_{ud}^* \sum_m C_m \, Q_m^{(0)} \tag{3.5}$$

where the summation is always finite, and we will drop the superscript (0) below. Eq. (3.5) illustrates that the local operators are weighted by effective couplings C_m called Wilson coefficients.

Let us now figure out explicitly what particular operators can arise from $\left(\bar{d}\,u\right)_{V-A}(\bar{c}\,b)_{V-A}$ after including effects of the strong interactions. Since these interactions are chirality-conserving, they cannot produce anything but the $(V-A)\times(V-A)$ structures at the dimension-six level. Moreover, the flavour content of all the operators must remain the same. Thus, it is only the color structure (i.e. contraction of the color indices) that may change with respect to our initial operator. We conclude that to all orders in QCD we have the following form of the Lagrangian

$$\mathcal{L}_{\text{eff}} = \frac{4G_F}{\sqrt{2}} \vee_{cb} V_{ud}^* \left(C_1 Q_1^{ducb} + C_2 Q_2^{ducb}\right), \tag{3.6}$$

where $Q_1^{ducb} = (\bar{d}_L^i \gamma^\mu u_L^j)(\bar{c}_L^j \gamma_\mu b_L^i)$, $Q_2^{ducb} = (\bar{d}_L^i \gamma^\mu u_L^i)(\bar{c}_L^j \gamma_\mu b_L^j)$, and i, j stand for color indices of the quark fields. Such operators are traditionally called current-current operators. Before turning on the QCD effects, we have $C_1 = 0$ and $C_2 = -1$.

Our operators can easily be rewritten in terms of products of color-singlet and color-octet currents, thanks to the following identity for the $SU(3)$ generators T^a:

$$(T^a)^i{}_j (T^a)^k_l = T_F \left(-\frac{1}{N_c}\delta^i_j \delta^k_l + \delta^i_l \delta^k_j\right) \tag{3.7}$$

where $T_F = 1/2$, and $N_c = 3$ stands for the number of quark colors. Moreover, one can

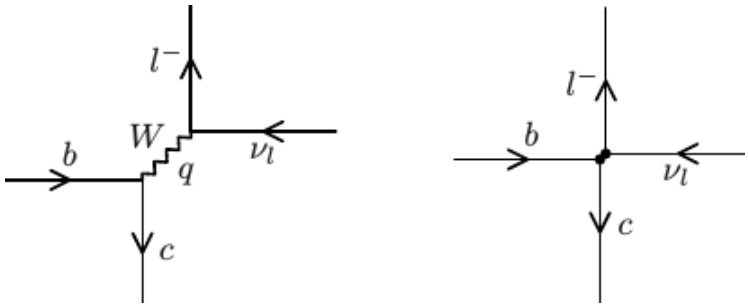

Figure 3.2: The LO $b \to cl\bar{\nu}_l$ process in the SM (left) and in the low energy effective theory (right). Black dots show an insertion of one of the effective operators. [40]

show that no other operators arise because there are only two independent singlets in the tensor product $\bar{\mathbf{3}} \otimes \mathbf{3} \otimes \bar{\mathbf{3}} \otimes \mathbf{3}$. The full set of operators in each given example can be written without specifying nothing but the particle content and symmetries of a given theory (see, e.g., Ref. [40]).

The effective Lagrangian for $b \to cl\bar{\nu}_l$ is given in Eq. 3.8 and depicted in fig. 3.2.

$$\mathcal{L}_{\text{eff}} = \frac{4G_F}{\sqrt{2}} \ \vee_{cb} (\bar{c}_L \gamma^\mu b_L)(\bar{l}_L \gamma_\mu \nu_L). \tag{3.8}$$

This lagrangian is extensively discussed in chapter 4 where the effective operator in the SM is defined as, $\mathcal{O}_V^{LL} = (\bar{c}\gamma_\mu P_L b)(\overline{\tau}\gamma^\mu P_L \nu_\tau) = (\bar{c}_L \gamma^\mu b_L)(\bar{l}_L \gamma_\mu \nu_L)$, where $P_L = (1-\gamma_5)/2$ and corresponding Wilson coefficients is $C_V^{LL} = 1$. The Hamiltonian for $b \to c\tau\bar{\nu}$ decay is given in Eq. 4.1. The SM lagrangian defined in Eq. 3.8 can be obtained from Eq. 4.1 by setting $C_{AB}^X = 0$.

We discuss theoretical framework for B physics in chapter 3. The effective Hamiltonian for $b \to c\tau\bar{\nu}$ decay can be generaly written as,

3.1.2 Determination and renormalization of the Wilson coefficients

The Wilson coefficients C_i in the effective theory Lagrangian 3.8 can be treated as coupling constants that undergo $\overline{\text{MS}}$ renormalization, similarly to the QCD gauge cou-

pling g_s. Once they are fixed at a given renormalization scale μ_0, their values at other scales μ can be calculated using the RGE. However, contrary to the gauge coupling, the initial conditions for the RGE ($C_i(\mu_0)$) do not need to be determined from experiment. Instead, they are fixed by the requirement that the effective theory in its region of validity reproduces the full theory (SM) Green's functions.

Instead of the SM, the role of the full theory could be played by any other model whose beyond-SM degrees of freedom are not much lighter than the W boson. In such a case, the operator basis in Eq. (3.8) might need to be extended. However, for definiteness, we shall restrict to the SM in our discussion here.

After solving the RGE, we calculate the physical amplitudes which are given by *matrix elements* of the operators Q_i between the final and initial states.

Such a procedure is common for any FCNC and FCCC process that takes place much below the electroweak scale. It always consists of three steps in which one subsequently determines the *matching*, *mixing* and *matrix elements*. A discussion of the matrix elements will follow in next Section.

3.1.3 Matrix elements

After having described the determination and renormalization of the Wilson coefficients, we now pass to the third step of the previously outlined procedure, namely to evaluating the matrix elements of the operators Q_i between the external P states of interest.

Due to the hadronic nature of the external states, nonperturbative QCD effects show up at the stage of the matrix element (unanimously called as Form Factors) evaluation. To overcome and/or control this problem, one considers the heavy quark limits, exploiting the fact that the b-quark mass is large compared to the QCD confinement scale δ. For exclusive decays, the available calculational frameworks are HQET [41], Soft-Collinear Effective Theory (SCET), QCD sum rules, light cone sum rules and lattice QCD. Matrix elements, $B \to D$ and $B \to D^*$, of our processes are discussed in

chapter 4. It is worthy to mention that for the inclusive decays, Heavy Quark expansion (HQE) allows to express the hadronic matrix elements in terms of the perturbative ones for the underlying quark-level process. In the following section we review HQET.

3.2 Heavy Quark Effective Theory (HQET)

HQET is a common feature of all EFTs with heavy quarks. HQET defines a single heavy quark system where all light degrees of freedom are soft, i.e. all their momenta's components are of the order δ_{QCD}. With the simplest heavy quark expansion, we will build its Lagrangian first from integrating out heavy degrees of freedom. Later we discuss symmetries of HQET that are very relevant feature of HQET for phenomenology, which eventually yield constraints on low scale non-perturbative matrix element that are not evident in full QCD.

3.2.1 Construction of the HQET Langrangian

To construct HQET's Lagrangian, the idea of EFT is directly followed by the identification of the heavy degree of freedom and the integrating it out from the functional integral. This approach is quite helpful, as it can be made explicitly at the tree level as well as at a one loop. This approach leads to the HQET Lagrangian being closed form, at least at tree level. The initial step is the QCD Lagrangian with a single heavy quark written as,

$$\mathcal{L}_{QCD} = \overline{Q}(i\not{D} - m_Q)Q + \mathcal{L}_{light}, \tag{3.9}$$

where m_Q is the mass of the heavy quark, $D_\mu = \partial_\mu + igA_\mu$ is the covariant derivative including the interaction with the gluon A_μ and $\mathcal{L}_{light}$ is the Langrangian for the light quarks and gluons. A decomposition of the covariant derivative into a 'time' and a 'spatial' ($\perp$) part,

$$D_\mu = v_\mu(v \cdot D) + D_\mu^\perp, \;\; D_\mu^\perp = (g_{\mu\nu} - v_\mu v_\nu)D^\nu, \;\; \{\not{D}^\perp, \not{v}\} = 0. \tag{3.10}$$

In order to calculate the HQET Langrangian suppose we have a single heavy quark system which is enclosed in the heavy hadron. This hadron has a mass m_H and moves with a definit momentum p_H. In case the hadron contains only a single heavy quark, its mass will scale with the heavy quark mass, likewise its momentum will scale with the heavy quark mass. To this end, it is convenient to define a four velocity

$$v = \frac{p_H}{m_H}, \qquad v^2 = 1, \qquad v_0 > 0, \tag{3.11}$$

which is independent of the heavy quark mass. This vector defines the desired frame $v = (1, 0, 0, 0)$ is the rest frame for heavy hadron. We consider heavy quark is inside the heavy hadron and

$$p_Q = m_Q v + k, \tag{3.12}$$

is the momentum of the heavy hadron where a small k *residual* momentum satisfying $k \ll m_Q$. To implement this idea on the technical side, we use this 'external' velocity vector v to decompose the heavy-quark field Q into an 'upper' (large) component ϕ and a 'lower' (or small) component ξ,

$$\phi_v = \frac{1}{2}(1 + \not{v})Q, \;\; \not{v}\phi_v = \phi, \;\; \xi_v = \frac{1}{2}(1 - \not{v})Q, \;\; \not{v}\xi_v = -\xi. \tag{3.13}$$

Using above new fields 3.13 and Eq. 3.10 in first part of Eq. 3.9 one finds,

$$\mathcal{L}_{heavy} = \overline{\phi}(i(v.D) - m_Q)\phi - \overline{\xi}(i(v.D) - m_Q)\xi + \overline{\phi}i\not{D}^{\perp}\phi + \overline{\xi}i\not{D}^{\perp}\xi. \tag{3.14}$$

To proceed further, we now implement the decomposition of the heavy quark momentum into a 'large' and a residual piece i.e., $p_Q = m_Q v + k$. This is achieved by multiplying the heavy quark field by a phase,

$$\phi_v = e^{-im_Q(v\cdot x)}h_v, \quad \xi_v = e^{-im_Q(v\cdot x)}H_v. \tag{3.15}$$

Since the momentum of a field is the derivative acting on the field that is,

$$p_Q^\mu \sim i\partial^\mu Q(x) \tag{3.16}$$

that leads us to obtain,

$$i\partial_\mu \phi_v(x) = e^{-im_Q(v\cdot x)}(m_Q v^\mu + i\partial^\mu)h_v, \tag{3.17}$$

which tells that the derivative acting on the field h_v reproduces the residual momentum k ($i\partial^\mu$) introduced above in Eq. 3.12. This observation give us with the power counting of HQET: once we have constructed the theory in terms of h_v , we aim at an expansion in $iD\mu/m_Q$.

Now one can indicate the Langrangian of the heavy quark in term of the field h_v and H_v as follows,

$$\mathcal{L}_{heavy} = \overline{h}_v i(v.D)h_v - \overline{H}_v\big\{i(v.D) + 2m_Q\big\}H_v + \overline{h}_v i\not{D}^\perp H_v + \overline{H}_v i\not{D}^\perp h_v. \tag{3.18}$$

With this formation of the Lagrangian we can now easily identify the degrees of freedom. In the sense of EFT, the field H_v is the heavy degree of freedom and field h_v is light. h_v does not have mass term and H_v has acquired a mass term $2m_Q$. The rest terms are couplings between these fields.

However, if the degree of freedom that has been integrated out is heavy, it is in general possible to expand the result in inverse powers of the mass of the heavy scale. In our case this is quite evident, since we have $(v \cdot D) \ll 2m_Q$ as $(v \cdot D)$ is related to the residual momentum k of the heavy quark. Consequently we expand and get,

$$\frac{1}{i(v\cdot D) + 2m_Q - i\epsilon} = \frac{1}{2m_Q}\sum_{n=0}^{\infty}\left(\frac{-i(v\cdot D)}{2m_Q}\right)^n. \tag{3.19}$$

Triming at some order N yields a local action functional, and hence we get as the

Lagranian,

$$\mathcal{L}_{1/m_Q\text{-}expansion} = \overline{h}_v i(v.D)h_v - \frac{1}{2m_Q}\overline{h}_v \not{D}^{\perp} \sum_{n=0}^{\infty} \left(\frac{-i(v\cdot D)}{2m_Q}\right)^n \not{D}^{\perp} h_v. \tag{3.20}$$

This expression is the expansion of the QCD Lagrangian up to the order $1/m_Q^N$. The leading term,

$$\mathcal{L}_{1/m_Q\text{-}expansion} = \overline{h}_v i(v.D)h_v, \tag{3.21}$$

is the Lagrangian for a static heavy quark moving with the four velocity v, i.e the Lagrangian on Heavy Quark Effective Theory (HQET).

The Feynman rules of HQET: The Feynmann rules of HQET are set up from the HQET Langrangian, [42]

$$\mathcal{L}_{HQET} = \overline{h}_v i(v.D)h_v = \overline{h}_v i(v.\partial)h_v + ig\overline{h}_v i(v.A)h_v. \tag{3.22}$$

The propagator may be read from in the first term, whereas the heavy quark-gluon interaction is represented in the second term as illustrated in Fig. 3.3.

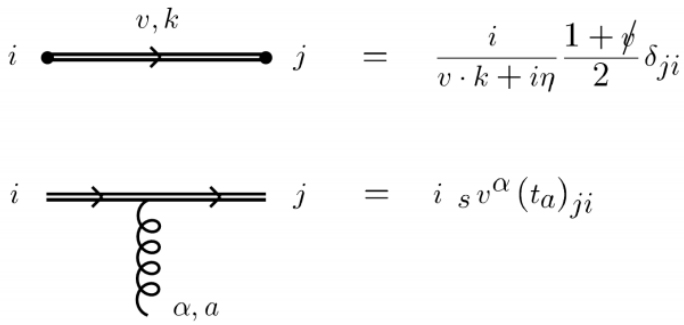

Figure 3.3: Feynmann rules of HQET. k is residual momentum moving with velocity v. i and j are the color indices. [42]

We will suppose the semileptonic decay $B \to Dl\overline{\nu}$ to illustrate this in more detail.

The corresponding hadronic matrix element is,

$$\langle B(p)\bar{b}\gamma_\mu cD(p')\rangle. \tag{3.23}$$

At scales below M_c, the static limit for both b and c quark can be used, however, the two mesons have different velocities $\upsilon = \frac{p}{M_b}$ and $\upsilon' = \frac{p'}{M_D}$, so we need to introduce two static quarks b_υ and c_υ with different velocities and we get the heavy quark Langrangian

$$\mathcal{L}^{b\to c}_{HQET} = \bar{b}_\upsilon i(\upsilon.D)b_\upsilon + \bar{c}_{\upsilon'} i(\upsilon'.D)c_{\upsilon'}, \tag{3.24}$$

where $v = p/M_b$ and $v' = p'/M_D$. Flavour Symmetry: QCD Lagrangian is familiar to have flavour symmetries in the event that quarks become mass degenerate: The approximate degeneracy of the quark relates to the isospin symmetry, in case all quarks are supposed to be massless, QCD has a chiral symmetry, of which the flavour $SU(3)$ is evident. It is because the interaction of quarks with gluons does not depend on mass, it depends on the color charge of the quarks represented in $SU(3)$. If a heavy quark is a static color source, its flavour becomes nsubstantial. To make this more clear, we consider the $b \to c$ HQET Langrangian for the case of two equal velocities,

$$\mathcal{L}^{b\to c}_{HQET} = \bar{b}_\upsilon i(\upsilon.D)b_\upsilon + \bar{c}_{\upsilon'} i(\upsilon^{'}.D)c_{\upsilon'}, \tag{3.25}$$

$$\mathcal{L}^{b\to c}_{HQET} = (\bar{b}_\upsilon, \bar{c}_\upsilon) \begin{pmatrix} i(\upsilon.D) & 0 \\ 0 & i(\upsilon.D) \end{pmatrix} \begin{pmatrix} b_\upsilon \\ c_\upsilon \end{pmatrix}, \tag{3.26}$$

which is as a model $SU(2)$ symmetry: for any unitary 2×2 matrix U transformation is defined as,

$$\begin{pmatrix} b_\upsilon \\ c_\upsilon \end{pmatrix}' = U \begin{pmatrix} b_\upsilon \\ c_\upsilon \end{pmatrix}, \tag{3.27}$$

under which the HQET Langraqngian stands invariant, this symmetry appeal only to

heavy quark moving at the same velocity v. We will suppose a semileptonic decay of B meson into a D meson and both b and c to be heavy. The maximum momentum transfer of the leptons defined as $q^2_{max} = (M_b - M_D)^2 = (M_b - M_c)^2$. Spin Symmetry: To make this intelligiable from the HQET Langrangian, we break down the heavy quark field into the two spin components by introducing a spin vector s with $s.v = 0$ and $s^2 = 0$ such that,

$$h_v^{\pm s} = \frac{1}{2}(1 \pm \gamma_5 \not{s}) h_v, \qquad h_v = h_v^{+s} + h_v^{-s}. \tag{3.28}$$

The expression in terms of the projections we have the Langrangian,

$$\mathcal{L}_{HQET} = \overline{h}_v^{+s}(iv D) h_v^{+s} + \overline{h}_v^{-s}(iv D) h_v^{-s}, \tag{3.29}$$

$$\mathcal{L}_{HQET} = (\overline{h}_v^{+s}, \overline{h}_v^{-s}) \begin{pmatrix} i(v.D) & 0 \\ 0 & i(v.D) \end{pmatrix} \begin{pmatrix} h_v^{+s} \\ h_v^{-s} \end{pmatrix}. \tag{3.30}$$

Similarly before we have an $SU(2)$ symmetry: for any 2×2 unitary matrix U transformation is defined as,

$$\begin{pmatrix} h_v^{+s} \\ h_v^{-s} \end{pmatrix}' = U \begin{pmatrix} h_v^{+s} \\ h_v^{-s} \end{pmatrix}, \tag{3.31}$$

under which the heavy quark symmetry remains invariant and symmetry relate again only heavy quarks moving with same velocity v.

Chapter 4

Analyses of $B \to D\tau\overline{\nu}_\tau$ and $B \to D^*\tau\overline{\nu}_\tau$

4.1 Theoretical framework

We discuss theoretical framework for B physics in chapter 3. The effective Hamiltonian for $b \to c\tau\bar{\nu}$ decay can be generaly written as,

$$\mathcal{H}_{\text{eff}} = \frac{4G_F \vee_{cb}}{\sqrt{2}} \left(\mathcal{O}^V_{LL} + \sum_{X=S,V,T;A,B=L,R} C^X_{AB}\, \mathcal{O}^X_{AB} \right), \tag{4.1}$$

that involve following ten four-fermion dimension six operators. S, V and T stands for scaler, vector and tensor, respectivly and L (R) represent P_L (P_R) defined in Eq. 2.2.

$$\begin{aligned} \mathcal{O}^V_{AB} &\equiv (\bar{c}\,\gamma^\mu P_A b)\,(\bar{\tau}\gamma_\mu P_B \nu)\ , \\ \mathcal{O}^S_{AB} &\equiv (\bar{c}\,P_A b)\,(\bar{\tau} P_B \nu)\ , \\ \mathcal{O}^T_{AB} &\equiv \lambda_{AB}\ (\bar{c}\,\sigma^{\mu\nu} P_A b)\,(\bar{\tau}\sigma_{\mu\nu} P_A \nu)\ , \end{aligned} \tag{4.2}$$

that includes right-handed leptonic part as well. λ_{AB} is kronecker delta function. Effective operator $\mathcal{O}^V_{LL}$ that only contribute in the SM is defined below Eq. 3.8. The SM contribution to $\mathcal{O}^V_{LL}$ is added to Eq. (4.1) such that $C^X_{AB} = 0$ in the SM. The non-zero C^X_{AB} is a manifestation of NP. It has been shown that NP in $b \to cl\bar{\nu}_l$ transitions [43] is

negligible therefore, we are assuming NP only in operators involving third generation charged leptons. In the following sections, we provide the analytic expressions of observables obtained from the $b \to c\tau\bar{\nu}_\tau$ quark-level decays. Our studies can be put into those involving $B \to D$ and $B \to D^*$ semileptonic decays.

4.2 $B \to D\tau\bar{\nu}_\tau$ decay transition

We study this process only in the SM. One can parametrize the hadronic matrix elements for $B \to D$ by showing explicitly their Lorentz structure as [44, 45],

$$\begin{aligned}
\langle D(p_D)|\bar{c}\gamma_\mu b|\bar{B}(p_B)\rangle &= \left[(p_B+p_D)_\mu - \frac{M_B^2-M_D^2}{q^2}q_\mu\right]F_1(q^2) + q_\mu\frac{M_B^2-M_D^2}{q^2}F_0(q^2)\,,\\
\langle D(p_D)|\bar{c}b|\bar{B}(p_B)\rangle &= \frac{M_B^2-M_D^2}{M_b-M_c}F_0(q^2)\,,\\
\langle D(p_D)|\bar{c}\gamma_\mu\gamma_5 b|\bar{B}(p_B)\rangle &= \langle D(p_D)|\bar{c}\gamma_5 b|\bar{B}(p_B)\rangle = 0\,,\\
\langle D(p_D)|\bar{c}\sigma_{\mu\nu} b|\bar{B}(p_B)\rangle &= -i(p_{B\mu}\,p_{D\nu} - p_{D\mu}\,p_{B\nu})\,\frac{2F_T(q^2)}{M_B+M_D}\,,\\
\langle D(p_D)|\bar{c}\sigma_{\mu\nu}\gamma_5 b|\bar{B}(p_B)\rangle &= -\epsilon_{\mu\nu\alpha\beta}\,p_B^\alpha\,p_D^\beta\,\frac{2F_T(q^2)}{M_B+M_D}\,,
\end{aligned} \tag{4.3}$$

where $F_0(q^2)$, $F_1(q^2)$ and $F_T(q^2)$ are the form factors in above matrix elements are defined as,

$$\begin{aligned}
F_1(q^2) &= \frac{1}{2\sqrt{M_BM_D}}\left[(M_B+M_D)\,h(q^2) - (M_B-M_D)\,h^{'}(q^2)\right],\\
F_0(q^2) &= \frac{1}{2\sqrt{M_BM_D}}\left[\frac{(M_B+M_D)^2-q^2}{M_B+M_D}\,h(q^2) - \frac{(M_B-M_D)^2-q^2}{M_B-M_D}\,h^{'}(q^2)\right],\\
F_T(q^2) &= \frac{M_B+M_D}{2\sqrt{M_BM_D}}\,h_T(q^2)\,.
\end{aligned} \tag{4.4}$$

In the heavy quark limit, each of above form factor either vanishes or equals to the leading order Isgur-Wise function,

$$h^{'} = 0, \qquad h = h_T = \xi. \tag{4.5}$$

The order $\mathcal{O}\left(\frac{\lambda_{\rm QCD}}{M_c}\right)$ corrections to form factors are calculated in [21]. We have not included above corrections in our analyses because our main focus is to discuss $B \to D^*\tau\bar{\nu}_\tau$ where we have consider HQET form factors.

4.2.1 Differential decay rate

The differential decay rate of $B \to D\tau\bar{\nu}_\tau$ can be written as,

$$\begin{aligned}
\frac{d\Gamma}{dq^2}(B \to D\tau\bar{\nu}) \;=\; & \frac{G_F^2 \vee_{cb}^2}{192 M_B^3 \pi^3}\, q^2\, \lambda_D^{1/2}(q^2) \left(1 - \frac{m_\tau^2}{q^2}\right)^2 \\
\times \; & \Bigg\{ \left(|1 + C_{LL}^V + C_{RL}^V|^2 + |C_{LR}^V + C_{RR}^V|^2\right) \left[(H_{V,0}^s)^2 \left(\frac{m_\tau^2}{2q^2} + 1\right) + \frac{3m_\tau^2}{2q^2}(H_{V,t}^s)^2\right] \\
& + \frac{3}{2}\,(H_S^s)^2 \Big(|C_{RL}^S + C_{LL}^S|^2 + |C_{RR}^S + C_{LR}^S|^2\Big) + 8\left(|C_{LL}^T|^2 + |C_{RR}^T|^2\Big)(H_T^s)^2 \left(1 + \frac{2m_\tau^2}{q^2}\right) \right. \\
& + 3\,\mathcal{R}\mathrm{e}\Big[(1 + C_{LL}^V + C_{RL}^V)\,(C_{RL}^S + C_{LL}^S)^* + (C_{LR}^V + C_{RR}^V)\,(C_{RR}^S + C_{LR}^S)^*\Big]\, \frac{m_\tau}{\sqrt{q^2}} H_S^s H_{V,t}^s \\
& \left. - 12\,\mathcal{R}\mathrm{e}\Big[(1 + C_{LL}^V + C_{RL}^V)\, C_{LL}^{T*} + (C_{RR}^V + C_{LR}^V)\, C_{RR}^{T*}\Big]\, \frac{m_\tau}{\sqrt{q^2}} H_T^s H_{V,0}^s \right\}. \qquad (4.6)
\end{aligned}$$

where the amplitudes for $B \to D$ transitions are:

$$\begin{aligned}
H_{V,0}^s(q^2) \;&\equiv\; H_{V_L,0}^s(q^2) \;=\; H_{V_R,0}^s(q^2) \;=\; \sqrt{\frac{\lambda_D(q^2)}{q^2}}\, F_1(q^2)\,, \\
H_{V,t}^s(q^2) \;&\equiv\; H_{V_L,t}^s(q^2) \;=\; H_{V_R,t}^s(q^2) \;=\; \frac{M_B^2 - M_D^2}{\sqrt{q^2}}\, F_0(q^2)\,, \\
H_S^s(q^2) \;&\equiv\; H_{S_L}^s(q^2) \;=\; H_{S_R}^s(q^2) \;\simeq\; \frac{M_B^2 - M_D^2}{M_b - M_c}\, F_0(q^2)\,, \qquad (4.7) \\
H_T^s(q^2) \;&=\; H_{T_L+-}^s = H_{T_L 0t}^s \;=\; -H_{T_R+-}^s = H_{T_R 0t}^s \;=\; -\frac{\sqrt{\lambda_D(q^2)}}{M_B + M_D}\, F_T(q^2)\,,
\end{aligned}$$

4.2.2 Plots

We obtained the plots for $B \to D$ process within the SM, $C_{AB}^X = 0$, that are shown in Figs. 4.1 and 4.2. The numerical value for input parameters that are used in our

calculation are given in Tab. 4.1 to make these plots. One can also obtain plots wrt

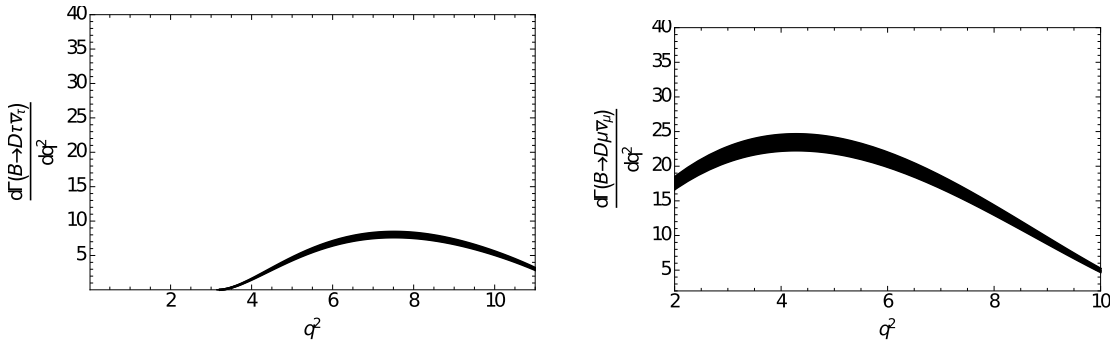

Figure 4.1: Differential decay rate in the SM for $B \to Dl\overline{\nu}_l$ with respect to q^2. Left plot is for τ and right plot is for μ. The band shows the parametric error.

to w that is defined as,

$$w \equiv v \cdot v' = \frac{(M_B^2 + M_D^2 - q^2)}{2M_B M_D}, \tag{4.8}$$

where v and v' are defined in HQET Sec. 3.2 and these plots within the SM are shown in Fig. 4.2.

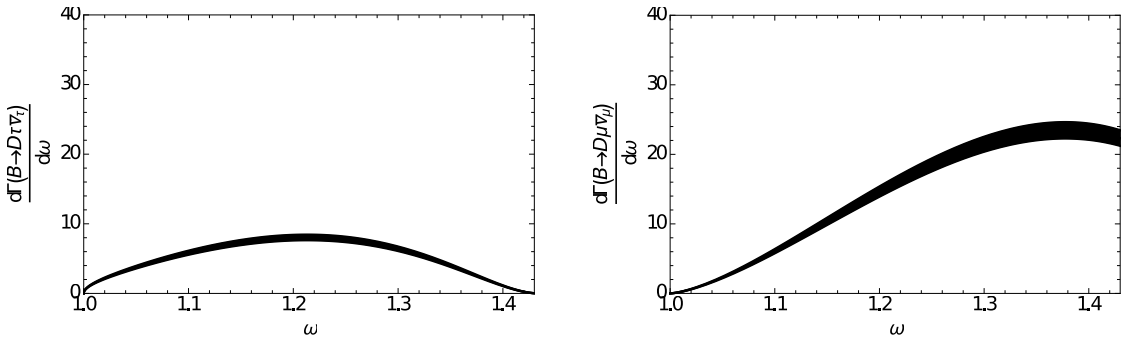

Figure 4.2: Differential decay rate in the SM for $B \to Dl\overline{\nu}_l$ with respect to Isgur-Wise function w. Left plot is for τ and right plot is for μ. The band around shows the parametric error.

4.3 $B \to D^* \tau \bar{\nu}_\tau$ decay transition

4.3.1 Matrix elements and Form Factors

The hadronic matrix elements for $B \to D^*$ transition are written as [44, 45],

$$\begin{aligned}
\langle D^*(p_{D^*},\lambda_M)|\bar{c}\gamma_\mu b|\bar{B}(p_B)\rangle &= -i\,\epsilon_{\mu\nu\zeta\sigma}\,\epsilon^{\nu *}(\lambda_M)\,p_B^\zeta\,p_{D^*}^\sigma\frac{2\,V(q^2)}{M_B+M_{D^*}}\,,\\
\langle D^*(p_{D^*},\lambda_M)|\bar{c}\gamma_\mu\gamma_5 b|\bar{B}(p_B)\rangle &= (M_B+M_{D^*})A_1(q^2)\left(\epsilon_\mu^*(\lambda_M)-q_\mu\frac{(\epsilon^*(\lambda_M)\cdot q)}{q^2}\right)\\
&\quad +q_\mu(\epsilon^*(\lambda_M)\cdot q)\frac{2M_{D^*}}{q^2}A_0(q^2)\\
&\quad -\frac{\epsilon^*(\lambda_M)\cdot q}{M_B+M_{D^*}}A_2(q^2)\left((p_B+p_{D^*})_\mu-q_\mu\frac{M_B^2-M_{D^*}^2}{q^2}\right),\\
\langle D^*(p_{D^*},\lambda_M)|\bar{c}b|\bar{B}(p_B)\rangle &= 0\,,\\
\langle D^*(p_{D^*},\lambda_M)|\bar{c}\gamma_5 b|\bar{B}(p_B)\rangle &= -(\epsilon^*(\lambda_M)\cdot q)\frac{2M_{D^*}}{M_b+M_c}A_0(q^2)\,,\\
\langle D^*(p_{D^*},\lambda_M)|\bar{c}\sigma_{\mu\nu} b|\bar{B}(p_B)\rangle &= \epsilon_{\mu\nu\zeta\sigma}\Big\{-\epsilon^{\zeta *}(\lambda_M)(p_B+p_{D^*})^\sigma T_1(q^2)\\
&\quad +2\frac{(\epsilon^*(\lambda_M)\cdot q)}{q^2}p_B^\zeta\,p_{D^*}^\sigma\left(T_1(q^2)-T_2(q^2)-\frac{q^2}{M_B^2-M_{D^*}^2}T_3(q^2)\right)\\
&\quad +\epsilon^{*\zeta}(\lambda_M)q^\sigma\frac{M_B^2-M_{D^*}^2}{q^2}(T_1(q^2)-T_2(q^2))\Big\}\,.
\end{aligned}\tag{4.9}$$

The $B \to D^*$ helicity amplitudes involving form factors for vector, axial, pseudoscalar currents,

$$\begin{aligned}
V(q^2) &= \frac{M_B+M_{D^*}}{2\sqrt{M_B M_{D^*}}}\,h_V(q^2),\\
A_1(q^2) &= \frac{(M_B+M_{D^*})^2-q^2}{2\sqrt{M_B M_{D^*}}(M_B+M_{D^*})}\,h_{A_1}(q^2),\\
A_2(q^2) &= \frac{M_B+M_{D^*}}{2\sqrt{M_B M_{D^*}}}\left[h_{A_3}(q^2)+\frac{M_{D^*}}{M_B}h_{A_2}(q^2)\right],\\
A_0(q^2) &= \frac{1}{2\sqrt{M_B M_{D^*}}}\left[\frac{(M_B+M_{D^*})^2-q^2}{2M_{D^*}}\,h_{A_1}(q^2)-\frac{M_B^2-M_{D^*}^2+q^2}{2M_B}\,h_{A_2}(q^2)\right.\\
&\qquad \left.-\frac{M_B^2-M_{D^*}^2-q^2}{2M_{D^*}}\,h_{A_3}(q^2)\right],
\end{aligned}\tag{4.10}$$

and for the tensor matrix elements read,

$$\begin{aligned}
T_1(q^2) &= \frac{1}{2\sqrt{M_B M_{D^*}}}\left[(M_B+M_{D^*})\,h_{T_1}(q^2)-(M_B-M_{D^*})\,h_{T_2}(q^2)\right],\\
T_2(q^2) &= \frac{1}{2\sqrt{M_B M_{D^*}}}\left[\frac{(M_B+M_{D^*})^2-q^2}{M_B+M_{D^*}}\,h_{T_1}(q^2)-\frac{(M_B-M_{D^*})^2-q^2}{M_B-M_{D^*}}\,h_{T_2}(q^2)\right], \qquad (4.11)\\
T_3(q^2) &= \frac{1}{2\sqrt{M_B M_{D^*}}}\left[(M_B-M_{D^*})\,h_{T_1}(q^2)-(M_B+M_{D^*})\,h_{T_2}(q^2)-2\,\frac{M_B^2-M_{D^*}^2}{M_B}\,h_{T_3}(q^2)\right].
\end{aligned}$$

The HQET form factors that we used in our work can be expressed as [46]

$$\begin{aligned}
h_V(w) =& R_1(w)h_{A_1}(w)\,,\\
h_{A_2}(w) =& \frac{R_2(w)-R_3(w)}{2\,r_{D^*}}h_{A_1}(w)\,,\\
h_{A_3}(w) =& \frac{R_2(w)+R_3(w)}{2}h_{A_1}(w)\,,\\
h_{T_1}(w) =& \frac{1}{2(1+r_{D^*}^2-2r_{D^*}w)}\left[\frac{M_b-M_c}{M_B-m_{D^*}}(1-r_{D^*})^2(w+1)\,h_{A_1}(w)\right.\\
&\left.-\frac{M_b+M_c}{M_B+m_{D^*}}(1+r_{D^*})^2(w-1)\,h_V(w)\right], \qquad (4.12)\\
h_{T_2}(w) =& \frac{(1-r_{D^*}^2)(w+1)}{2(1+r_{D^*}^2-2r_{D^*}w)}\left[\frac{M_b-M_c}{M_B-m_{D^*}}\,h_{A_1}(w)-\frac{M_b+M_c}{M_B+m_{D^*}}\,h_V(w)\right],\\
h_{T_3}(w) =& -\frac{1}{2(1+r_{D^*})(1+r_{D^*}^2-2r_{D^*}w)}\left[2\frac{M_b-M_c}{M_B-m_{D^*}}r_{D^*}(w+1)\,h_{A_1}(w)\right.\\
&-\frac{M_b-M_c}{M_B-m_{D^*}}(1+r_{D^*}^2-2r_{D^*}w)(h_{A_3}(w)-r_{D^*}h_{A_2}(w))\\
&\left.-\frac{M_b+M_c}{M_B+m_{D^*}}(1+r_{D^*})^2\,h_V(w)\right],
\end{aligned}$$

where the w-dependencies are parametrized as [46]

$$\begin{aligned} h_{A_1}(w) =& h_{A_1}(1)[1 - 8\zeta^2_{D^*} z + (53\zeta^2_{D^*} - 15)z^2 - (231\zeta^2_{D^*} - 91)z^3] \,, \\ R_1(w) =& R_1(1) - 0.12(w-1) + 0.05(w-1)^2 \,, \\ R_2(w) =& R_2(1) + 0.11(w-1) - 0.06(w-1)^2 \,, \\ R_3(w) =& 1.22 - 0.052(w-1) + 0.026(w-1)^2 \,, \end{aligned} \tag{4.13}$$

where $r_{D^*} = M_{D^*}/M_B$,$w = (M_B^2 + M_{D^*}^2 - q^2)/2M_B M_{D^*}$, $z(w) = (\sqrt{w+1} - \sqrt{2})/(\sqrt{w+1} + \sqrt{2})$. The numerical values of the parameters that we used in form factors are given as,

$$h_{A_1}(1) = 0.908 \pm 0.017 \quad [47], \qquad \zeta^2_{D^*} = 1.207 \pm 0.026 \quad [48], \tag{4.14}$$

$$R_1(1) = 1.403 \pm 0.033 \quad [48], \qquad R_2(1) = 0.854 \pm 0.020 \quad [48] \,. \tag{4.15}$$

4.3.2 Four fold angular distribution

In this decay, the vector meson D^* in the final state as shown in Fig. 4.3 provides additional observables as compare to the $B \to D$ case. The differential decay distribution of this decay process $B(p_B) \to D^*(p_{D^*})\, \tau(p_\tau)\, \bar{\nu}(p_{\bar{\nu}})$, with $D^*(p_{D^*}) \to D(p_D)\, \pi(p_\pi)$ on the mass shell, can be expressed in the form [49],

$$\begin{aligned} \frac{d^4\Gamma(B \to D^* \tau \bar{\nu})}{dq^2\, d\cos\theta_l\, d\cos\theta^*\, d\chi} \;\equiv\; & I(q^2, \theta_l, \theta^*, \chi) \\ =\; & \frac{9}{32\pi} \Big\{ I_1^s \sin^2\theta^* + I_1^c \cos^2\theta^* + \left(I_2^s \sin^2\theta^* + I_2^c \cos^2\theta^*\right) \cos 2\theta_l \\ & + (I_3 \cos 2\chi + I_9 \sin 2\chi) \sin^2\theta^* \sin^2\theta_l + (I_4 \cos\chi + I_8 \sin\chi) \sin 2\theta^* \sin 2\theta_l \\ & + (I_5 \cos\chi + I_7 \sin\chi) \sin 2\theta^* \sin\theta_l + \left(I_6^s \sin^2\theta^* + I_6^c \cos^2\theta^*\right) \cos\theta_l \Big\} \end{aligned} \tag{4.16}$$

The angular coefficients I_i's that depends on q^2 contain both short- and long-distance

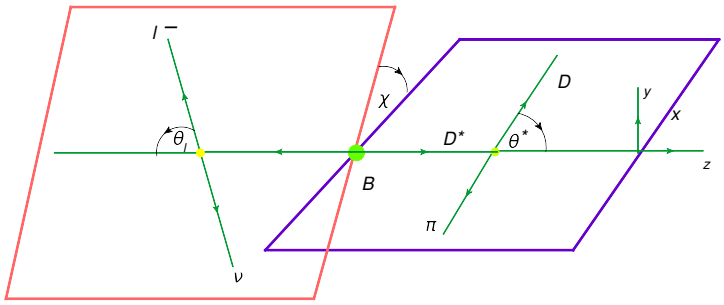

Figure 4.3: The description of the angles in the four fold angular distribution. [49]

physics contributions. Using the global normalization,

$$N_F = \frac{G_F^2 \,|\, \vee_{cb} \,|^2}{2^7\, 3\pi^3 m_B^3}\, q^2\, \lambda_{D^*}^{1/2}(q^2) \left(1 - \frac{m_\tau^2}{q^2}\right)^2 \mathcal{B}(D^* \to D\pi)\,, \tag{4.17}$$

where $\mathcal{B}(D^* \to D\,\pi)$ is the branching fraction of the D^* decay into $D\,\pi$ states, the expressions for the angular coefficients are,

$$\begin{aligned}
I_1^c &= N_F \left[2\left(1 + \frac{m_\tau^2}{q^2}\right)\left(|\mathcal{A}_0^L|^2 + 4\,|\mathcal{A}_{T\,0}^L|^2\right) - \frac{16 m_\tau}{\sqrt{q^2}}\,\mathcal{R}\mathrm{e}[\mathcal{A}_0^L \mathcal{A}_{T\,0}^{L*}] + \frac{4m_\tau^2}{q^2}\,|A_{tP}^L|^2 + (L \to R)\right], \\
I_1^s &= N_F \left[\frac{1}{2}\left(3 + \frac{m_\tau^2}{q^2}\right)\left(|\mathcal{A}_\perp^L|^2 + |\mathcal{A}_\parallel^L|^2\right) + 2\left(1 + \frac{3m_\tau^2}{q^2}\right)\left(|\mathcal{A}_{T\,\perp}^L|^2 + |\mathcal{A}_{T\,\parallel}^L|^2\right)\right. \\
&\qquad \left. - 8\,\frac{m_\tau}{\sqrt{q^2}}\,\mathcal{R}\mathrm{e}[\mathcal{A}_\perp^L \mathcal{A}_{T\,\perp}^{L\,*} + \mathcal{A}_\parallel^L \mathcal{A}_{T\,\parallel}^{L*}] + (L \to R)\right], \\
I_2^c &= -2\,N_F \left(1 - \frac{m_\tau^2}{q^2}\right)\left(|\mathcal{A}_0^L|^2 - 4\,|\mathcal{A}_{T\,0}^L|^2 + (L \to R)\right), \\
I_2^s &= \frac{1}{2}\,N_F \left(1 - \frac{m_\tau^2}{q^2}\right)\left(|\mathcal{A}_\perp^L|^2 + |\mathcal{A}_\parallel^L|^2 - 4\left(|\mathcal{A}_{T\,\perp}^L|^2 + |\mathcal{A}_{T\,\parallel}^L|^2\right) + (L \to R)\right), \\
I_3 &= N_F \left(1 - \frac{m_\tau^2}{q^2}\right)\left(|\mathcal{A}_\perp^L|^2 - |\mathcal{A}_\parallel^L|^2 - 4\left(|\mathcal{A}_{T\,\perp}^L|^2 - |\mathcal{A}_{T\,\parallel}^L|^2\right) + (L \to R)\right), \\
I_4 &= \sqrt{2}\,N_F \left(1 - \frac{m_\tau^2}{q^2}\right)\mathcal{R}\mathrm{e}[\mathcal{A}_0^L \mathcal{A}_\parallel^{L*} - 4\,\mathcal{A}_{T\,0}^L \mathcal{A}_{T\,\parallel}^{L*} + (L \to R)]\,,
\end{aligned}$$

$$
\begin{aligned}
I_5 &= 2\sqrt{2}\, N_F \Big[\mathcal{R}\mathrm{e}[\big(\mathcal{A}_0^L - 2\,\frac{m_\tau}{\sqrt{q^2}}\,\mathcal{A}_{T\,0}^L\big)\,\big(\mathcal{A}_\perp^{L\,*} - 2\,\frac{m_\tau}{\sqrt{q^2}}\,\mathcal{A}_{T\,\perp}^{L^*}\big) - (L\to R)] \\
&\qquad - \frac{m_\tau^2}{q^2}\,\mathcal{R}\mathrm{e}[A_{tP}^{L^*}\,\big(\mathcal{A}_\parallel^L - 2\,\frac{\sqrt{q^2}}{m_\tau}\mathcal{A}_{T\,\parallel}^L\big) + (L\to R)]\Big]\,, \\
I_6^c &= N_F\,\frac{8m_\tau^2}{q^2}\,\mathcal{R}\mathrm{e}[A_{tP}^{L^*}\,\big(\mathcal{A}_0^L - 2\,\frac{\sqrt{q^2}}{m_\tau}\,\mathcal{A}_{T\,0}^L\big) + (L\to R)]\,, \\
I_6^s &= 4\,N_F\,\mathcal{R}\mathrm{e}[\big(\mathcal{A}_\parallel^L - 2\,\frac{m_\tau}{\sqrt{q^2}}\,\mathcal{A}_{T\,\parallel}^L\big)\big(\mathcal{A}_\perp^{L\,*} - 2\frac{m_\tau}{\sqrt{q^2}}\mathcal{A}_{T\,\perp}^{L^*}\big) - (L\to R)]\,, \\
I_7 &= -2\sqrt{2}\,N_F\Big[\mathcal{I}\mathrm{m}[\big(\mathcal{A}_0^L - 2\,\frac{m_\tau}{\sqrt{q^2}}\,\mathcal{A}_{T\,0}^L\big)\,\big(\mathcal{A}_\parallel^{L^*} - 2\,\frac{m_\tau}{\sqrt{q^2}}\,\mathcal{A}_{T\,\parallel}^{L^*}\big) - (L\to R)] \\
&\qquad + \frac{m_\tau^2}{q^2}\,\mathcal{I}\mathrm{m}[A_{tP}^{L^*}\,\big(\mathcal{A}_\perp^L - 2\,\frac{\sqrt{q^2}}{m_\tau}\,\mathcal{A}_{T\,\perp}^L\big) + (L\to R)]\Big]\,, \\
I_8 &= \sqrt{2}\,N_F\,\Big(1 - \frac{m_\tau^2}{q^2}\Big)\,\mathcal{I}\mathrm{m}[\mathcal{A}_0^{L^*}\mathcal{A}_\perp^L - 4\,\mathcal{A}_{T\,0}^{L^*}\mathcal{A}_{T\,\perp}^L + (L\to R)]\,, \\
I_9 &= 2\,N_F\,\Big(1 - \frac{m_\tau^2}{q^2}\Big)\,\mathcal{I}\mathrm{m}[\mathcal{A}_\parallel^L\mathcal{A}_\perp^{L\,*} - 4\,\mathcal{A}_{T\,\parallel}^L\mathcal{A}_{T\,\perp}^{L^*} + (L\to R)]\,.
\end{aligned}
\tag{4.18}
$$

where the $\mathcal{A}_\lambda^{L,R}$ are the transversity amplitudes, that are the projections of the total decay amplitude into the explicit polarization basis. Their explicit dependence on the hadronic helicity amplitudes, and the Wilson coefficients is listed below,

$$
\begin{aligned}
\mathcal{A}_0^L &= H_{V,0}\;(1 + C_{LL}^V - C_{RL}^V), & \mathcal{A}_0^R &= H_{V,0}\;(C_{LR}^V - C_{RR}^V), \\
\mathcal{A}_\parallel^L &= \frac{1}{\sqrt{2}}\,(H_{V,+} + H_{V,-})\;(1 + C_{LL}^V - C_{RL}^V), & \mathcal{A}_\parallel^R &= \frac{1}{\sqrt{2}}\,(H_{V,+} + H_{V,-})\;(C_{LR}^V - C_{RR}^V), \\
\mathcal{A}_\perp^L &= \frac{1}{\sqrt{2}}\,(H_{V,+} - H_{V,-})\;(1 + C_{LL}^V + C_{RL}^V), & \mathcal{A}_\perp^R &= \frac{1}{\sqrt{2}}\,(H_{V,+} - H_{V,-})\;(C_{LR}^V + C_{RR}^V), \\
\mathcal{A}_t^L &= H_{V,t}\;(1 + C_{LL}^V - C_{RL}^V), & \mathcal{A}_t^R &= H_{V,t}\;(C_{LR}^V - C_{RR}^V), \\
\mathcal{A}_P^L &= H_S\;(C_{RL}^S - C_{LL}^S), & \mathcal{A}_P^R &= H_S\;(C_{RR}^S - C_{LR}^S), \\
\mathcal{A}_{T0}^L &= 2H_{T,0}\;C_{LL}^T, & \mathcal{A}_{T0}^R &= -2H_{T,0}\;C_{RR}^T, \\
\mathcal{A}_{T\parallel}^L &= \sqrt{2}\,(H_{T,+} - H_{T,-})\;C_{LL}^T, & \mathcal{A}_{T\parallel}^R &= -\sqrt{2}\,(H_{T,+} - H_{T,-})\;C_{RR}^T, \\
\mathcal{A}_{T\perp}^{L,R} &= \sqrt{2}\,(H_{T,+} + H_{T,-})\;C_{LL}^{T,R}\,,
\end{aligned}
\tag{4.19}
$$

where the t and the P amplitudes combined as

$$\mathcal{A}_{tP}^{L,R} = \left(\mathcal{A}_{t}^{L,R} + \frac{\sqrt{q^2}}{m_\tau}\,\mathcal{A}_{P}^{L,R}\right). \tag{4.20}$$

The hadronic helicity amplitudes are,

$$\begin{aligned}
H_{V,\pm}(q^2) &= (M_B + M_{D^*})\,A_1(q^2) \mp \frac{\sqrt{\lambda_{D^*}(q^2)}}{M_B + M_{D^*}}\,V(q^2)\,,\\
H_{V,0}(q^2) &= \frac{M_B + M_{D^*}}{2M_{D^*}\sqrt{q^2}}\left[-(M_B^2 - M_{D^*}^2 - q^2)\,A_1(q^2) + \frac{\lambda_{D^*}(q^2)}{(M_B + M_{D^*})^2}\,A_2(q^2)\right],\\
H_{V,t}(q^2) &= -\sqrt{\frac{\lambda_{D^*}(q^2)}{q^2}}\,A_0(q^2)\,,\\
H_{S}(q^2) &= -\frac{\sqrt{\lambda_{D^*}(q^2)}}{M_b + M_c}\,A_0(q^2)\,,\\
H_{T,0}(q^2) &= \frac{1}{2M_{D^*}}\left[-(M_B^2 + 3\,M_{D^*}^2 - q^2)\,T_2(q^2) + \frac{\lambda_{D^*}(q^2)}{M_B^2 - M_{D^*}^2}\,T_3(q^2)\right],\\
H_{T\pm}(q^2) &= \frac{1}{\sqrt{q^2}}\left[\pm(M_B^2 - M_{D^*}^2)\,T_2(q^2) + \sqrt{\lambda_{D^*}}\,T_1(q^2)\right].
\end{aligned} \tag{4.21}$$

4.3.3 Observables

We define observables as follows,

- Differential decay rate

$$\frac{d\Gamma}{dq^2} = \frac{1}{4}\left(3I_{1c} + 6I_{1s} - I_{2c} - 2I_{2s}\right), \tag{4.22}$$

- R_{D^*}

$$R_{D^*} \equiv \frac{d\Gamma(B \to D^*\tau\overline{\nu}_\tau)/dq^2}{d\Gamma(B \to D^* l\overline{\nu}_l)/dq^2}, \tag{4.23}$$

- Forward-backward asymmetry

$$A_{\rm FB}(q^2) = \frac{3}{8}\frac{(I_{6c} + 2I_{6s})}{d\Gamma/dq^2}\,, \tag{4.24}$$

- D^* polarization fraction

$$R_{L,T}(q^2) = \frac{d\Gamma_L/dq^2}{d\Gamma_T/dq^2}\,, \tag{4.25}$$

where Γ_L and Γ_T are the longitudinal and transverse D^* polarization decay rates,

$$\frac{d\Gamma_L}{dq^2} = \frac{1}{4}\left(3I_{1c} - I_{2c}\right)\,, \qquad \frac{d\Gamma_T}{dq^2} = \frac{1}{2}\left(3I_{1s} - I_{2s}\right)\,. \tag{4.26}$$

Alternatively, one can define the quantity $F_L^{D^*}$ which is a measure of the longitudinally polarized D^*'s as,

$$F_L^{D^*}(q^2) = \frac{R_{L,T}(q^2)}{1 + R_{L,T}(q^2)} = \frac{1}{2}\,\frac{3I_{1c} - I_{2c}}{3\left(I_{1c} + I_{1s}\right) - I_{2c} - I_{2s}}\,. \tag{4.27}$$

$F_L^{D^*}$ is also labelled as $F_L^{D^*}(q^2)$ integrated over the available phase space.

- $R_{A,B}$

$$R_{A,B}(q^2) = \frac{d\Gamma_A/dq^2}{d\Gamma_B/dq^2}\,, \tag{4.28}$$

$$\frac{d\Gamma_A}{dq^2} = \frac{1}{4}\left(I_{1c} + 2I_{1s} - 3I_{2c} - 6I_{2s}\right)\,, \qquad \frac{d\Gamma_B}{dq^2} = \frac{1}{2}\left(I_{1c} + 2I_{1s} + I_{2c} + 2I_{2s}\right)\,. \tag{4.29}$$

- A_3 and A_9

$$A_3(q^2) = \frac{1}{2\pi}\frac{I_3}{d\Gamma/dq^2}\,, \qquad A_9(q^2) = \frac{1}{2\pi}\frac{I_9}{d\Gamma/dq^2}\,. \tag{4.30}$$

- A_4 and A_8

$$A_4(q^2) = -\frac{2}{\pi}\frac{I_4}{d\Gamma/dq^2}\,, \qquad A_8(q^2) = \frac{2}{\pi}\frac{I_8}{d\Gamma/dq^2}\,. \tag{4.31}$$

- A_5 and A_7

$$A_5(q^2) = -\frac{3}{4}\frac{I_5}{d\Gamma/dq^2}\,, \qquad A_7(q^2) = -\frac{3}{4}\frac{I_7}{d\Gamma/dq^2}\,. \tag{4.32}$$

- A_{6s}

$$A_{6s}(q^2) = -\frac{27}{8}\frac{I_{6s}}{d\Gamma/dq^2}\,. \tag{4.33}$$

The observables A_7, A_8 and A_9 that are proportional to I_7, I_8 and I_9, respectively are zero in the SM. We have not shown plots for these observables in Fig. 4.6.

The numerical value for input parameters that are used in our calculation are given in Tab. 4.1 to make plots in Secs. 4.2.2 and 4.3.4.

Table 4.1: The numerical value for input parameters that are used in our calculation.

$M_b = 5.28$ GeV	$M_D = 1.86$ GeV	$m_{D^*} = 2.01$ GeV
$\xi = 1$	$\vee_{cb} = 39.8{\cdot}10^{-3}$	$G_F = 1.166 \cdot 10^{-5}$ GeV^{-2}
$m_\mu = 0.1057$ GeV	$m_\tau = 1.7768$ GeV	$M_b = 4.18$
$M_c = 1.27$ GeV		

4.3.4 Plots

Plots for Eq. 4.22 within the SM are shown in Figs. 4.4 and 4.5. The numerical value for input parameters that are used in our calculation are given in Tab. 4.1 to make these plots. One can also obtain plots wrt to w that is defined as,

$$w \;\equiv v \cdot v' = \frac{(M_B^2 + M_{D^*}^2 - q^2)}{2M_B M_{D^*}} \tag{4.34}$$

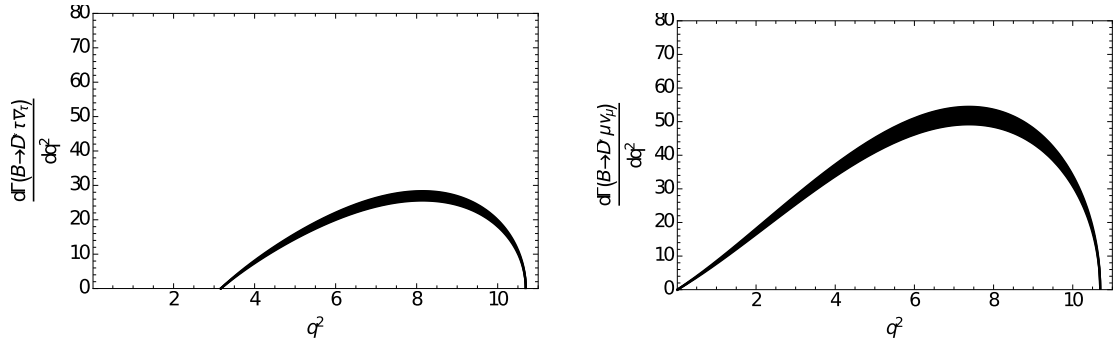

Figure 4.4: Differential decay rate in the SM for $B \to D^* l\overline{\nu}_l$ with respect to function q^2. Left plot is for τ and right plot is for μ. The band shows the parametric error.

where v and v' are defined in HQET Sec. 3.2 and these plots within the SM are shown in Fig. 4.5. The plots of other q^2-dependent observables defined above for different

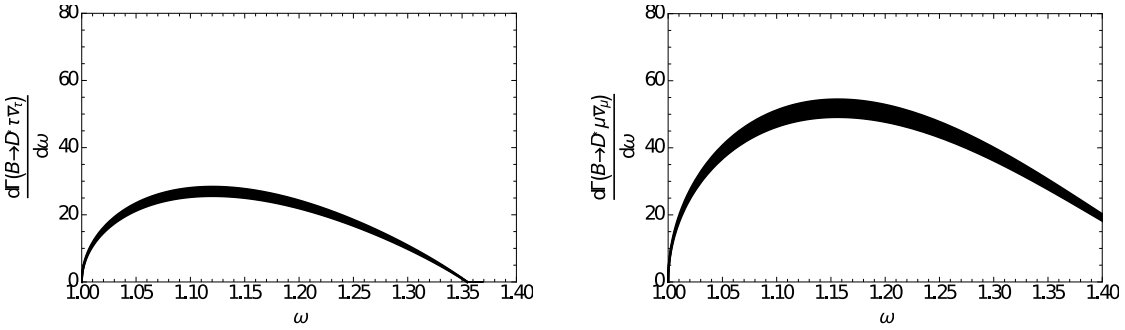

Figure 4.5: Differential decay rate in the SM for $B \to D^* l\overline{\nu}_l$ with respect to Isgur-Wise function w. Left plot is for τ and right plot is for μ. The band shows the parametric error.

benchmark values of NP couplings are shown in Fig. 4.6.

To make plots we took the benchmark values of g_i from Ref. [49] that read as follows,

$$g_V = 0.20 \pm i0.19, \qquad g_S = 0.17 \pm i0.16, \qquad g_A = 0.69 \pm i1.04,$$
$$g_P = 0.58 \pm i0.21, \qquad g_T = 0.21 \pm i0.35, \tag{4.35}$$

where

$$g_{V,A} = g_{V_R} \pm g_{V_L}, \qquad g_{S,P} = g_{S_R} \pm g_{S_L}, \qquad g_T = g_{T_L}. \tag{4.36}$$

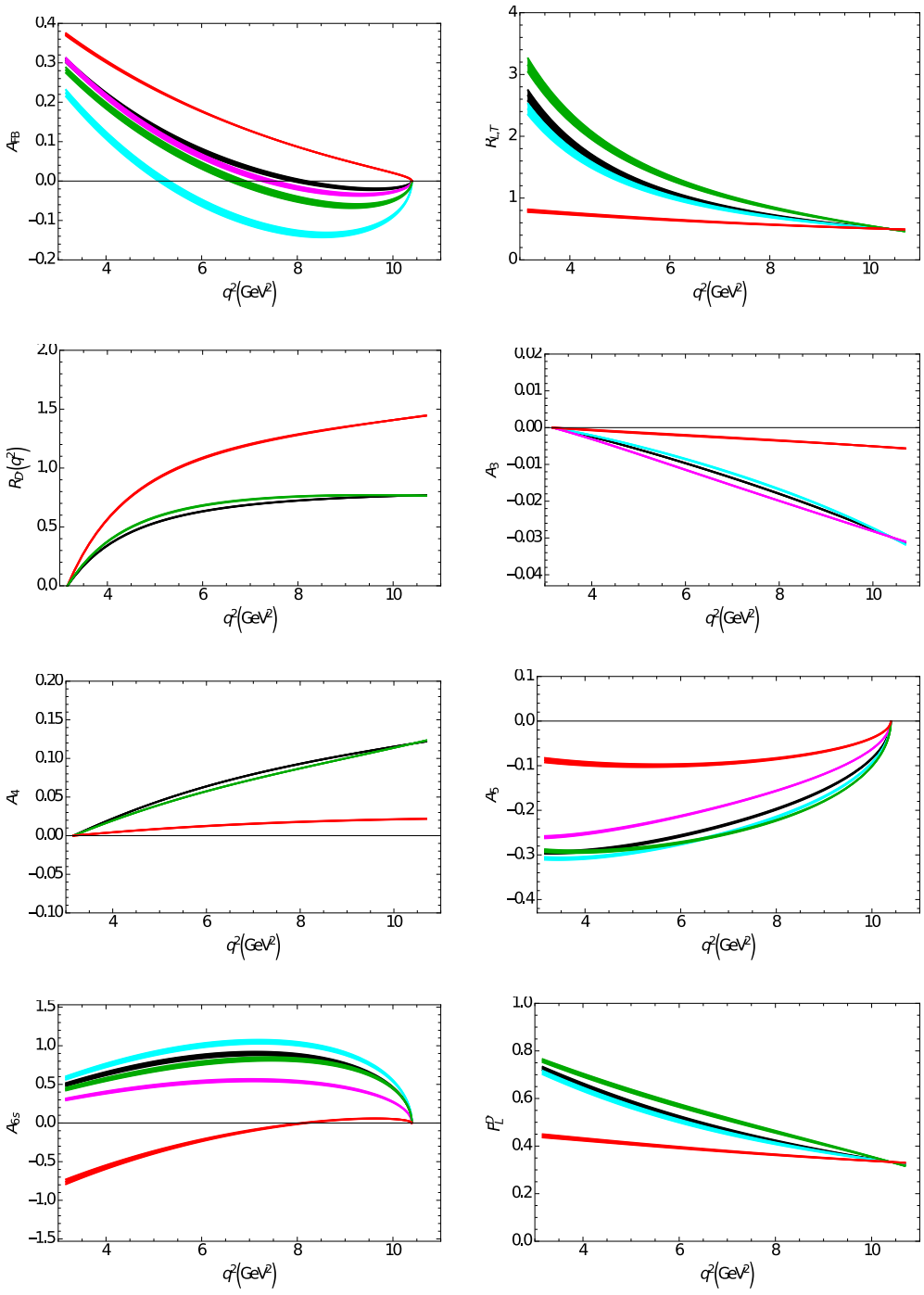

Figure 4.6: Observables for NP couplings g_i and as functions of q^2. The width of each curve shows the theoretical uncertainties in hadronic form factors and quark masses. The benchmark g_i are given in Eq. 4.35 are the best fit values. Black, cyan, purple, green and red curves are for the SM, g_V, g_A, g_P and g_T values, respectively.

The Wilson coefficients C_{AB}^{X} in Eq. 4.1 are linked with coupling defined in Eq. 4.36 as follows,

$$g_{V_L} = C_{LL}^{V}, \qquad g_{V_R} = C_{RL}^{V}, \qquad g_{S_L} = C_{RL}^{S},$$
$$g_{S_R} = C_{RL}^{S}, \qquad g_{T_L} = C_{LL}^{T}. \tag{4.37}$$

Our plots match with the Fig. 2 of Ref. [49]. Our value of R_{D^*} in the SM that we have evaluated reads as,

$$R_{D^*} = 0.257 \pm 0.003. \tag{4.38}$$

The average SM values of I_i are defined as

$$\langle I_i \rangle_\ell \;=\; \frac{1}{\Gamma(B \to D^* \ell \bar{\nu}_\ell)} \times \int_{m_\ell^2}^{(M_B - m_{D^*})^2} I_i^\ell(q^2)\, dq^2 \tag{4.39}$$

that for tau leptons in the final state, are given in Tab. 4.2.

ℓ	$\langle I_{1c} \rangle_\ell$	$\langle I_{1s} \rangle_\ell$	$\langle I_{2c} \rangle_\ell$	$\langle I_{2s} \rangle_\ell$	$\langle I_3 \rangle_\ell$	$\langle I_4 \rangle_\ell$	$\langle I_5 \rangle_\ell$	$\langle I_{6c} \rangle_\ell$	$\langle I_{6s} \rangle_\ell$	$\langle I_7 \rangle_\ell$	$\langle I_8 \rangle_\ell$	$\langle I_9 \rangle_\ell$
τ	0.56(1)	0.346(4)	-0.145(2)	0.054(1)	-0.088(1)	-0.138(1)	0.290(5)	0.36(2)	-0.26(1)	0	0	0

Table 4.2: Standard Model values of the coefficients appearing in the angular distribution, integrated over the full available phase space, as indicated in Eq. (4.39). The values are obtained by using the HQET form factors.

Chapter 5

Conclusions

We study $B \to D\tau\bar{\nu}_\tau$ and $B \to D^*\tau\bar{\nu}_\tau$ flavour changing charged current processes. These decay processes are interesting due to having persistent anomalies, R_D and R_{D^*}, reported by the different experiment like LHCb, Belle and BABAR. These anomalies hint physics beyond the standard model. For theoretical framework to study these transitions, we adopt an effective field theory approach and write a low-energy effective Hamiltonian for all possible dimension-six operators including new physics. We used the corresponding Wilson coefficients obtained from a numerical fit to all available experimental data to predict our observables. For numerical predictions we used HQET form factors for both transitions. We study in detail the four fold angular distribution for $B \to D^*\tau\bar{\nu}$ that provides interesting angular observables. Our findings match with the known results [49] within and beyond the standard model in the model independent way for observables including angular observables.

Bibliography

[1] S. L. Glashow, *Partial Symmetries Of Weak Interactions*, Nucl. Phys. **22** (1961) 579.

[2] S. Weinberg, *A Model Of Leptons*, Phys. Rev. Lett. **19** (1967) 1264.

[3] A. Salam, *Weak And Electromagnetic Interactions*, Originally printed in 'Svartholm: Elementary Particle Theory, Proceedings Of The Nobel Symposium Held 1968 At Lerum, Sweden', Stockholm 1968, 367-377.

[4] M. Gell-Mann, *A Schematic Model Of Baryons And Mesons*, Phys. Lett. **8** (1964) 214.

[5] M. Y. Han and Y. Nambu, *Three-triplet model with double SU(3) symmetry*, Phys. Rev. B **139** (1965) 1006.

[6] D. J. Gross and F. Wilczek, *Ultraviolet Behavior of Non-abelian Gauge Theories*, Phys. Rev. Lett. **30** (1973) 1343.

[7] H. D. Politzer, *Reliable Perturbative Results for Strong Interactions?*, Phys. Rev. Lett. **30** (1973) 1346.

[8] S. Weinberg, *Nonabelian Gauge Theories Of The Strong Interactions*, Phys. Rev. Lett. **31** (1973) 494.

[9] H. Fritzsch, M. Gell-Mann and H. Leutwyler, *Advantages Of The Color Octet Gluon Picture*, Phys. Lett. B **47** (1973) 365.

[10] P.W. Higgs, *Broken symmetries and the masses of gauge bosons*, Phys. Rev. Lett. **13** (1964) 508.

[11] G. S. Guralnik, C. R. Hagen, and T. W. B. Kibble, *Global conservation laws and massless particles*, Phys. Rev. Lett. **13** (1964) 585.

[12] F. Englert and R. Brout, *Broken symmetry and the mass of gauge vector mesons*, Phys. Rev. Lett. **13** (1964) 321.

[13] P. W. Higgs, *Spontaneous Symmetry Breakdown without Massless Bosons*, Phys. Rev. **145** (1966) 1156.

[14] T. W. B. Kibble, *Symmetry breaking in non-Abelian gauge theories*, Phys. Rev. **155** (1967) 1554.

[15] G. 't Hooft, *Renormalization of Massless Yang-Mills Fields*, Nucl. Phys. B **33** (1971) 173.

[16] G. 't Hooft, *Renormalizable Lagrangians for massive yang-mills fields*, Nucl. Phys. B **35** (1971) 167.

[17] ATLAS Collaboration, G. Aad *et al.*, *Combined search for the Standard Model Higgs boson using up to* 4.9 fb^{-1} *of pp collision data at* $\sqrt{s} = 7$ *TeV with the ATLAS detector at the LHC*, Phys. Lett. B **710** (2012) 49 [arXiv:1202.1408].

[18] CMS Collaboration, S. Chatrchyan *et al.*, *Combined results of searches for the standard model Higgs boson in pp collisions at* $\sqrt{s} = 7$ *TeV*, Phys. Lett. B **710** (2012) 26 [arXiv:1202.1488].

[19] *Measurements of* R_D *and* R_{D^*} at Belle II, Hülya Atmacan University of Cincinnati Belle September 23, 2020

[20] D. Bigi and P. Gambino, Phys. Rev. D **94** (2016) no.9, 094008 [arXiv:1606.08030 [hep-ph]].

[21] F. U. Bernlochner, Z. Ligeti, M. Papucci and D. J. Robinson, Phys. Rev. D **95** (2017) no.11, 115008 [arXiv:1703.05330 [hep-ph]].

[22] D. Bigi, P. Gambino and S. Schacht, JHEP **11** (2017), 061 [arXiv:1707.09509 [hep-ph]].

[23] S. Jaiswal, S. Nandi and S. K. Patra, JHEP **12** (2017), 060 [arXiv:1707.09977 [hep-ph]].

[24] Y. Amhis *et al.* [HFLAV], Eur. Phys. J. C **77** (2017) no.12, 895 [arXiv:1612.07233 [hep-ex]].

[25] A. Matyja *et al.* [Belle], Phys. Rev. Lett. **99** (2007), 191807 [arXiv:0706.4429 [hep-ex]].

[26] A. Bozek *et al.* [Belle], Phys. Rev. D **82** (2010), 072005 [arXiv:1005.2302 [hep-ex]].

[27] M. Huschle *et al.* [Belle], Phys. Rev. D **92** (2015) no.7, 072014 [arXiv:1507.03233 [hep-ex]].

[28] Y. Sato *et al.* [Belle], Phys. Rev. D **94** (2016) no.7, 072007 [arXiv:1607.07923 [hep-ex]].

[29] S. Hirose *et al.* [Belle], Phys. Rev. D **97** (2018) no.1, 012004 [arXiv:1709.00129 [hep-ex]].

[30] J. P. Lees *et al.* [BaBar], Phys. Rev. Lett. **109** (2012), 101802 [arXiv:1205.5442 [hep-ex]].

[31] R. Aaij *et al.* [LHCb], Phys. Rev. Lett. **115** (2015) no.11, 111803 [arXiv:1506.08614 [hep-ex]].

[32] R. Aaij *et al.* [LHCb], Phys. Rev. D **97** (2018) no.7, 072013 [arXiv:1711.02505 [hep-ex]].

[33] *The Standard Model Higgs BosonPart of the Lecture Particle Physics II*, UvA Particle Physics Master 2013-2014

[34] N. Cabibbo, *Unitary symmetry and leptonic decays*, Phys. Rev. Lett. **10** (1963) 531.

[35] M. Kobayashi and T. Maskawa, *CP Violation In The Renormalizable Theory Of Weak Interaction*, Prog. Theor. Phys. **49** (1973) 652.

[36] E. Stueckelberg, A. Petermann, *La normalisation des constantes dans la theorie des quanta*, Helv. Phys. Acta. **26** (1953) 499;

[37] T. Appelquist and J. Carazzone, *Infrared Singularities and Massive Fields*, Phys. Rev. D **11** (1975) 2856.

[38] K. G. Wilson, *Nonlagrangian Models Of Current Algebra*, Phys. Rev. **179** (1969) 1499.

[39] W. Zimmermann, *Normal Products And The Short Distance Expansion In The Perturbation Theory Of Renormalizable Interactions*, Annals Phys. **77** (1973) 570.

[40] B. Grzadkowski, M. Iskrzynski, M. Misiak, J. Rosiek, *Dimension-Six Terms in the Standard Model Lagrangian*, JHEP **1010** (2010) 085 [arXiv:1008.4884].

[41] N. Isgur and M. B. Wise, *Weak Decays of Heavy Mesons in the Static Quark Approximation*, Phys. Lett. B **232** (1989) 113; *Weak Transition Form-factors Between Heavy Mesons*, Phys. Lett. B **237** (1990) 527.

[42] Lectures at Les Houches 2017, Thomas Mannel *Theoretische Elementarteilchenphysik*, Naturwiss.- techn. Fakultät, Universität Siegen, **57068** Siegen, Germany

[43] M. Jung and D. M. Straub, "Constraining new physics in $b \to c\ell\nu$ transitions," *JHEP* **01** (2019) 009, `arXiv:1801.01112 [hep-ph]`.

[44] Y. Sakaki, M. Tanaka, A. Tayduganov, and R. Watanabe, "Testing leptoquark models in $\bar{B} \to D^{(*)}\tau\bar{\nu}$," *Phys. Rev.* **D88** no. 9, (2013) 094012, `arXiv:1309.0301 [hep-ph]`.

[45] C. Murgui, A. Peñuelas, M. Jung, and A. Pich, "Global fit to $b \to c\tau\nu$ transitions," *JHEP* **09** (2019) 103, arXiv:1904.09311 [hep-ph].

[46] I. Caprini, L. Lellouch and M. Neubert, Nucl. Phys. B **530**, 153 (1998) [hep-ph/9712417].

[47] J. A. Bailey *et al.* [Fermilab Lattice and MILC Collaborations], Phys. Rev. D **89**, no. 11, 114504 (2014) [arXiv:1403.0635 [hep-lat]].

[48] Y. Amhis *et al.* [Heavy Flavour Averaging Group (HFAG)], arXiv:1412.7515 [hep-ex].

[49] Bečirević, Damir and Fedele, Marco and Nišandžić, Ivan and Tayduganov, Andrey, arXiv:1907.02257 [hep-ph].